

# **Insulin-coated titanium implants – a potential therapy for local bone regeneration**

Behnosh Öhrnell Malekzadeh

Department of Orthodontics  
Institute of Odontology  
Sahlgrenska Academy at University of Gothenburg



UNIVERSITY OF GOTHENBURG

Gothenburg 2017

Cover illustration: Microcomputer tomography images of a rat tibia (Source: Behnosh Öhrnell Malekzadeh).

Insulin-coated titanium implants – a potential therapy for local bone regeneration

© Behnosh Öhrnell Malekzadeh 2017

behnosh.malekzadeh@gu.se

ISBN 978-91-629-0149-3 (print), 978-91-629-0150-9 (PDF).

<http://hdl.handle.net/2077/51877>

Printed in Gothenburg, Sweden 2017

Ineko AB

“När plan A misslyckas har vi alltid resten av alfabetet”

Loesje



# ABSTRACT

**Background:** Insulin is a hormone that regulates glucose metabolism, however, it is also important for bone formation. The anabolic effect of insulin on bone could open up alternative therapies when it comes to local bone regeneration. However, this requires a method for local administration of insulin.

**Aim:** The overall aim was to determine whether local administration of insulin, coated on a titanium surface has the potential to regenerate bone locally.

**Materials and methods:** The surface characteristics and release kinetics of the insulin coating were analysed by interferometry, ellipsometry, SEM, XPS, and ECLIA. The biological activity of the released insulin was evaluated *in vitro*, in osteoblast-like cells (MG-63), by a Neutral Red and alizarin red assay. The gene expression and bone formation in healthy and ovariectomised rats were evaluated using quantitative real-time PCR, microcomputer tomography, and histomorphometry.

**Results:** The insulin-coated titanium surface showed a smooth surface topography on a micrometer level and the coating generated a heterogeneous protein layer. The insulin coating demonstrated a high initial release, with the release continuing over a 6-week period. Titanium surface modifications, increased coating thickness, and incubation in serum-enriched cell culture medium increased the amount of insulin release, while storage decreased the amount of insulin release. When serum-enriched medium was used, the insulin was partially substituted by serum proteins. The remaining insulin layer had direct surface effects by stabilising the structures of protein competitors and supporting the precipitation of CaP on the surface. The released insulin retained its biological activity, as demonstrated by a significant increase in cell number and mineralisation capacity. Insulin-coated implants increased local bone formation in healthy rat tibias, decreased the expression of the early pro-inflammatory cytokine interleukin-1 $\beta$ , and increased periosteal bone formation in osteoporotic rats.

**Conclusion:** An insulin-coated titanium implant surface represents a potential therapy for local bone regeneration.

**Keywords:** Insulin, titanium, bone, implant, osteoblast, immobilisation

**ISBN:** 978-91-629-0149-3 (print), 978-91-629-0150-9 (PDF).

# SAMMANFATTNING PÅ SVENSKA

**Bakgrund:** Insulin är ett hormon som reglerar glukosmetabolismen, men som även är viktigt för benbildningsprocesser. Insulinets positiva effekt på benbildning öppnar möjligheter för alternativa terapier för lokal benregeneration. Det behövs dock en metod för lokal administration av insulin.

**Syfte:** Det övergripande syftet var att undersöka om administration av insulin från en titanyta kan vara en potentiell terapi för lokal benregeneration.

**Material och metoder:** Ytegenskaper och avgivningskinetik för de insulinbelagda titanytorna analyserades med interferometri, ellipsometry, SEM, XPS och ECLIA. Det avgivna insulinets biologiska aktivitet analyserades i humana osteoblaster (MG-63) med Neutral Red upptag och alizarin red färgning. Det lokalt administrerade insulinets effekt på genuttryck och benbildning analyserades med kvantitativ real-time PCR, mikrodatorrtografi och histomorfometri i friska och ovariektomerade råttor.

**Resultat:** Den insulinbelagda titanytan uppvisade en slät yttopografi på mikrometer nivå med ett heterogent proteinlager. Insulinet avgavs från titanytan med en hög initial avgivning som avtog under en 6 veckors period. Ytmodifiering av titanytan, ökning av insulintjockleken samt inkubation i cellodlings medium med serum ökade avgivningen medan förvaring av diskarna minskade avgivningen. Vid inkubation i cellodlingsmedium med serum skedde ett utbyte av insulin och serumproteiner. Det kvarvarande insulinlagret stabiliserade sammansättningen av de konkurrerande proteinerna från serum samt medierade CaP precipitation på ytan. Det avgivna insulinet uppvisade bibehållen biologisk aktivitet genom att cellantal och mineralisationskapacitet ökade. Insulinbelagda titanimplantat ökade lokal benbildningen i friska råttor och minskade genuttrycket av det proinflammatoriska cytokinet interleukin-1 $\beta$  samt ökade den periostala benbildningen i osteoporotiska råttor.

**Konklusion:** Den insulinbelagda titanimplantatyten representerar en potentiell terapi för lokal benregeneration.

# LIST OF PAPERS

This thesis is based on the following studies, referred to in the text by their Roman numerals.

- I. Malekzadeh B, Tengvall P, Ohnrell LO, Wennerberg A, Westerlund A. Effects of locally administered insulin on bone formation in non-diabetic rats. *J Biomed Mater Res A*. 2013 Jan;101(1):132-7.
- II. Malekzadeh BÖ, Ransjö M, Tengvall P, Mladenovic Z, Westerlund A. Insulin released from titanium discs with insulin coatings – Kinetics and biological activity. *J Biomed Mater Res B Appl Biomater*. 2016 May 26. doi: 10.1002/jbm.b.33717
- III. Shchukarev A, Malekzadeh BÖ, Ransjö M, Tengvall P, Westerlund A. Surface characterization of insulin-coated Ti6Al4V medical implants conditioned in cell culture medium: An XPS study. *Journal of Electron Spectroscopy and Related Phenomena*. 2017 April;216:33-38. doi:<http://dx.doi.org/doi:10.1016/j.elspec.2017.03.001>
- IV. Malekzadeh BÖ, Erlandsson MC, Tengvall P, Palmqvist A, Ransjö M, Bokarewa MI, Westerlund A. Effects of locally administered insulin on bone formation in osteoporotic rats. Submitted.

The original papers are reprinted with permission from the respective publishers.

# CONTENTS

ABBREVIATIONS .....	IV
1 INTRODUCTION .....	1
1.1 Rationale.....	1
1.2 Bone .....	3
1.2.1 Skeletal bones.....	3
1.2.2 Bone structure.....	4
1.2.3 Bone cells .....	5
1.2.4 Bone formation.....	7
1.2.5 Bone healing.....	8
1.2.6 Bone remodelling .....	9
1.2.7 Pathological bone remodelling.....	11
1.3 Insulin.....	13
1.3.1 An osteoanabolic hormone .....	15
1.4 Titanium and osseointegration .....	18
1.4.1 Titanium surface modification .....	19
1.4.2 Protein surface modification.....	20
2 OVERALL AIM.....	23
2.1 Specific aims .....	23
3 MATERIALS AND METHODS .....	24
3.1 Implant and sample preparation .....	25
3.1.1 Implants .....	25
3.1.2 Cleaning procedure.....	25
3.1.3 Immobilisation technique .....	25
3.1.4 The insulin coating .....	27
3.2 Surface analysis.....	27
3.2.1 Interferometry.....	27
3.2.2 Ellipsometry .....	28
3.2.3 Scanning electron microscopy.....	29

3.2.4	X-ray photo-electron spectroscopy .....	29
3.3	<i>In vitro</i> study methods .....	29
3.3.1	Electro-chemiluminescence immunoassay .....	29
3.3.2	Cells and cell culturing .....	30
3.3.3	Neutral Red uptake assay.....	30
3.3.4	Mineralisation assay by Alizarin Red staining .....	31
3.4	<i>In vivo</i> study methods.....	31
3.4.1	Animals.....	31
3.4.2	Surgery.....	32
3.4.3	Blood glucose measurement .....	34
3.4.4	Micro-computer tomography.....	34
3.4.5	Histology and histomorphometry .....	35
3.4.6	Quantitative Real-Time PCR.....	35
3.5	Statistical analysis .....	37
3.6	Ethical approvals .....	37
4	RESULTS .....	38
4.1	Study I .....	38
4.2	Study II.....	38
4.3	Study III.....	40
4.4	Study IV .....	41
4.5	Pilot study.....	42
5	DISCUSSION .....	45
6	CONCLUSIONS.....	52
7	REFERENCES .....	53
8	ACKNOWLEDGEMENTS .....	64

# ABBREVIATIONS

AGE	Advanced glycation end-products
Akt	Protein kinase B
ALP	Alkaline phosphatase
APTES	Aminopropyltriethoxysilane
BMP	Bone morphogenetic proteins
BA	Bone area
BIC	Bone-to-implant contact
BMD	Bone mineral density
BMU	Bone multinuclear unit
C3, C5	Complement factor 3, 5
Casp8	Caspase 8
CatK	Cathepsin K
Col-1	Collagen type I
CP	Commercially pure
DM	Diabetes mellitus
ECLIA	Electro-chemiluminescence immune analysis assay
EDC	N-(3-dimethyl aminopropyl)-N'-ethylcarbodiimide
ER $\alpha$	Oestrogen receptor alpha
ERK	Extracellular signalling regulated kinase
FGF	Fibroblast growth factor
GA	Glutaraldehyde
HA	Hydroxyapatite
IDE	Insulin-degrading enzyme
IGF-I, II	Insulin-like growth factor-I, II
IL-1 $\beta$	Interleukin-1beta
IL-6	Interleukin-6
IL-10	Interleukin-10
I $\kappa$ B	Inhibitor of nuclear factor-kappa B

IRS	Insulin receptor substrate
MAPK	Mitogen-activated protein kinase
M-CSF	Macrophage colony-stimulating factor
MMPs	Matrix metalloproteinases
MSC	Mesenchymal stem cells
NF- $\kappa$ B	Nuclear factor-kappa B
NHS	N-Hydroxysulfosuccinimide sodium salt
NR	Neutral red
PDGF	Platelet-derived growth factor
PECAM-1	Platelet and endothelial cell adhesion molecule-1
PI3K	Phosphatidylinositide 3-kinase
PTH	Parathyroid hormone
OPG	Osteoprotegerin
OCN	Osteocalcin
Osx	Osterix
Ovx	Ovariectomised
qPCR	Quantitative polymerase chain reaction
RANKL	Receptor activator of nuclear factor-kappa B ligand
RANK	Receptor activator of nuclear factor-kappa B
ROS	Reactive oxygen species
Runx2	Runt-related transcription factor-2
SAM	Self-assembling monolayers
SEM	Scanning electron microscopy
TGF- $\beta$	Transforming growth factor-beta
TNF- $\alpha$	Tumour necrosis factor-alpha
TRAP	Tartrate-resistant acid phosphatase
VEGF	Vascular endothelial growth factor
WNT	Wingless-type MMTV integration site family
XPS	X-ray photo-electron spectroscopy



# 1 INTRODUCTION

## 1.1 Rationale

Development of biomaterials used for bone regeneration is a rapidly growing area of research. In medical technology, knowledge of material surfaces is used to engineer surface modifications, which can change the biological responses to the material. In a population that has longer life expectancy, increased incidence of bone related diseases, and stringent demands for positive treatment outcomes, the use of biomaterials (i.e. titanium), that could regulate bone formation is of great interest. However, controlling bone formation is a major challenge, as numerous substances regulate the complex process of bone cell signalling, with many of the components still unknown.

Titanium is commonly used in medicine for bone-anchored prostheses such as teeth<sup>1,2</sup>, hearing aids<sup>3</sup>, hip<sup>4</sup>, extremity<sup>5</sup>, and the fixation of fractured bone fragments, orthognatic and reconstructive surgery<sup>6,7</sup>. Even though titanium is mostly successfully used in these cases, complex bone defects and compromised bone quality remain as significant challenges. In 2014, 31,500 patients received 78,000 dental implants in Sweden (Swedish Social Insurance Agency). Recent studies of the effectiveness of dental implants, analysed in a randomly chosen Swedish population, showed the loss of at least one implant in 7.6% of the studied patients<sup>8</sup>. Moreover, approximately 17,000 patients undergoes hip replacement surgeries in Sweden each year; 5%–10% of which will undergo a revision during the life-time of the recipient<sup>9</sup>. The risk of failure is higher for revision surgery and bone grafting is needed more often for these patients<sup>9,10</sup>. Even though the treatment of hip fractures with intramedullary or extramedullary fixation is associated with high success rates, approximately 10% of the patients (mostly the oldest patients) suffer from complications, requiring revision interventions, which are linked to high mortality and morbidity. One of the most common complications is the perforation of the hip joint by the lag screw (i.e., cut-out), which is very painful and disabling<sup>11</sup>. Pseudarthrosis or “false joint” is still the most common type of failure after spinal fusion, and the literature reports an incidence of pseudarthrosis in the range of 0%–56%<sup>12-14</sup>.

To meet these challenges and to improve the treatment modalities, there is a need to devise therapies that stimulate bone formation at the afflicted site, for example with an osteoinductive, large-scale reproducible and

inexpensive substance. In this thesis, the surface of a titanium implant is coated with the hormone insulin, this to avoid the induction of the systemic endocrine effect, while taking advantage of the local osteoanabolic effect of insulin.

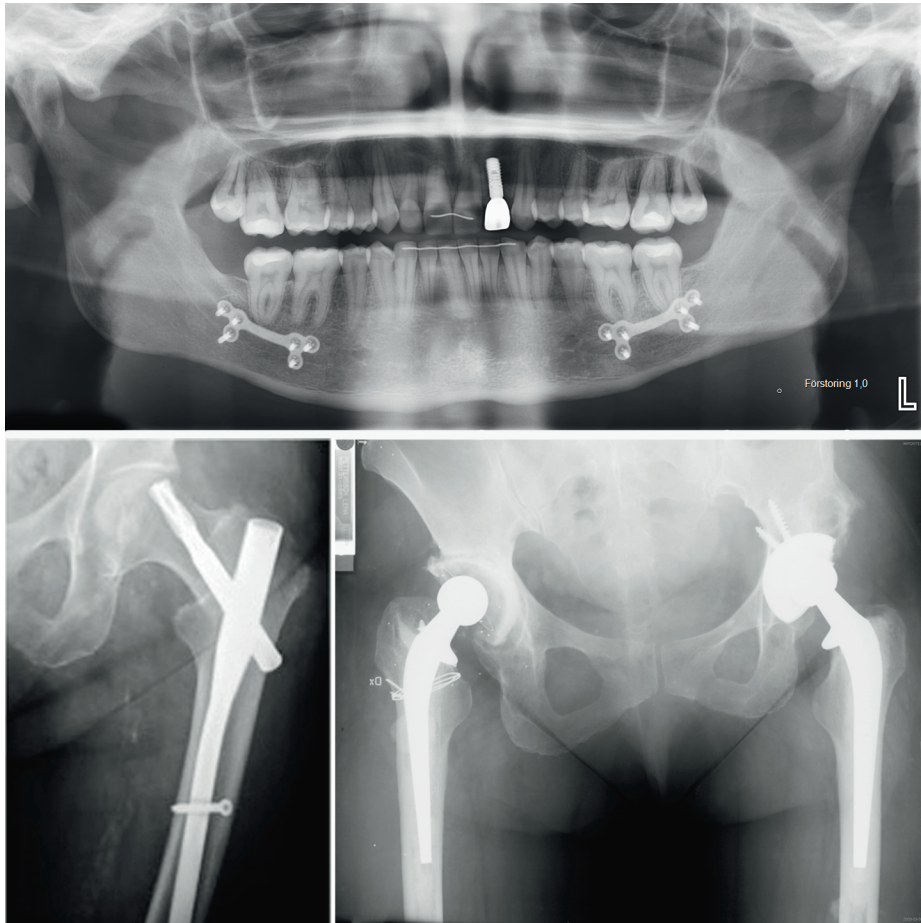


*Figure 1. X-ray images of (upper panel): dental implant for tooth replacement and titanium fixation plates after orthognatic surgery, (lower-left panel); intramedullary fixation of a femoral fracture with a cut-out complication, and (lower-right panel); patient with bilateral total hip arthroplasties with a cemented hip prosthesis (left) and a non-cemented hip prosthesis (right). Courtesy of Lars-Olof Öhrnell, Alicja Bojan, Mahziar Mohaddes, respectively.*

## 1.2 Bone

Bone is a highly specialised connective tissue that consists of several types of cells; osteoblasts, osteocytes, bone-lining cells, and osteoclasts. The extracellular matrix consists of 65% of the wet bone weight of organic components (i.e., osteoid), 25% inorganic components (i.e., mineral crystals), and 10% water, which give the tissue its mechanical strength and flexibility. The main functions of bone are: Providing support and protection; facilitating locomotion; acting as a reservoir of growth factors; formation of blood and immune cells; and maintaining mineral homeostasis<sup>15-17</sup>.

Bone is involved in the mineral homeostasis and acts as a reservoir for phosphate and calcium ions. Mineral homeostasis refers to the concentrations of phosphate and especially calcium ions in the extracellular fluid, which are crucial for the body to function normally. Systems that are dependent upon calcium ions include those involved in the transmission of nerve impulses, muscle contraction, and blood coagulation<sup>17,18</sup>. If the calcium levels in the blood are altered, the body will respond by releasing parathyroid hormone (PTH), which is produced by the parathyroid glands or calcitonin, which is produced by the thyroid gland. These molecules in combination with 1,25-dihydroxyvitamin D<sub>3</sub> restore normal mineral homeostasis<sup>19,20</sup>. The mineral homeostasis regulates the serum levels of minerals rather than the health of the bone tissue, even though it is integrated in the remodelling process<sup>17,18</sup>. PTH is released when the calcium levels are decreased and it stimulates osteoclast-mediated bone resorption and renal calcium resorption from the kidney, in order to increase the levels of calcium ions in the blood. Subsequently, 1,25-dihydroxyvitamin D<sub>3</sub> increases calcium absorption from the intestine<sup>18,20</sup>. However, intermittent usage of PTH is known to increase bone formation and, therefore, the drug teriparatide (a recombinant form of the first amino acid sequences of parathyroid hormone) is used for osteoporosis therapy<sup>21</sup>. In contrast, calcitonin inhibits osteoclast bone resorption but plays a smaller role in the regulation of the physiologic calcium level in adult humans<sup>17,18,22</sup>.

### 1.2.1 Skeletal bones

The skeletal bones in vertebrates can be classified based on localisation or form. Regarding localisation, the appendicular skeleton supports the appendages, while the axial skeleton comprises the bones of the head and torso. A more common way to categorise bone is based on form, i.e., short, flat, long, and irregular types of bone. Short bone (e.g., tarsals and carpals) is

characterised by its size; it has the same dimension in all directions. In contrast, flat bone (e.g., cranial bones, scapula, mandible, and sternum) and long bone have one dimension that is longer than the others. Long bones (e.g., femur, tibia, humerus, metacarpals, metatarsals and phalanges) are more or less cylindrical and have three regions: Diaphysis, metaphysis, and epiphysis. Irregular bone (e.g., vertebra and maxilla) is characterised by its non-uniform shape<sup>16,23</sup>.

## 1.2.2 Bone structure

The macro-architecture of the bone tissue is divided into the trabecular (also known as spongy or cancellous bone) and compact (also known as hard or cortical bone) types. Trabecular bone represents 20% of the total skeletal mass, while cortical bone represents the remaining 80%. The internal and external surfaces of bone are lined with layers of cells, called the endosteum and periosteum, respectively<sup>15,16</sup>. The periosteum, which is a thin innervated and vascularised membrane, consists of an outer fibrous layer and an inner cambrium layer that contains progenitor cells and osteoblasts<sup>24</sup>. The outer layer also consists of Sharpey's fibres or perforating fibres, which are bundles of collagen type I fibres that connect the periosteum to the bone. In animal studies, it has been demonstrated that removal of the periosteum dramatically affects bone healing<sup>25</sup>. At specific sites between the bone trabeculae, the red bone marrow is found, which contains multipotent stem cells and the site of production of red and white blood cells. Even though trabecular and compact bones have similar matrix composition and structure, they differ in mass, in that trabecular bone has a lower mass-to-volume ratio<sup>16</sup>. Thus, trabecular bone is associated with higher metabolic activity, while compact bone is associated with greater mechanical strength. Trabecular and compact bones can be either woven (primary) or lamellar (secondary). Woven bone, which has a scattered, irregular structure, is seen in embryonic bones and during the early phase of fracture healing, and it is subsequently remodelled to bone that has a more organised structural arrangement<sup>16,26,27</sup>.

The micro-architecture of bone tissue consists of 'packets' in trabecular bone (semi-lunar form) and 'Haversian systems' in cortical bone (cylindrical form). Since the trabecular packets have no central canal with blood vessels, they are remodelled exclusively from the outer surface. Haversian systems or osteon units consist of concentric sheets (lamellae) arranged around a central canal that contains blood vessels, lymph vessels, and nerves. Interstitial

lamella is found between the osteons, while circumferential lamella is found in the outer layer of the bone. Volkmann's canals are located between the central canals and the circumferential lamellae. Tunnel-like structures (called 'canaliculi') are responsible for communication and transportation of nutrition to the osteocytes trapped between the osteons. Consequently, bone is a highly dynamic tissue in which signalling and communication are occurring continuously. On the outer border of each osteon there is a cement line, which separates the lamellae. The canaliculi and collagen fibrils do not cross this cement line. If a crack in the bone matrix develops it tends to follow the cement line rather than extend across the osteons<sup>15,16,23,28</sup>.

### 1.2.3 Bone cells

Bone cells are either bone-forming or bone-resorbing cells based on their origin. Osteoblasts, osteocytes, and bone-lining cells originate from mesenchymal stem cells (MSC), whereas osteoclasts originate from hematopoietic stem cells. Their locations also differ, with osteoblasts, osteoclasts, and bone-lining cells being found along the bone surface, while osteocytes are entrapped in the bone matrix<sup>27-29</sup>.

#### Osteoblasts

Osteoblasts originate from multipotent MSC located in the bone marrow, endosteum, and periosteum. The recruitment and differentiation of mesenchymal cells are crucial steps in bone formation. Runx-related transcription factor 2 (Runx2) is a key molecule in the cellular signal transduction pathway that directs progression towards the osteogenic lineage. Osterix (Osx) is another transcription factor that is important for osteogenesis, and it is suggested to work down-stream of Runx2<sup>23,29</sup>. The mechanism by which the pre-osteoblasts develop to a mature osteoblast is complex and is dependent upon multiple signalling molecules, including bone morphogenic proteins (BMP), WNT proteins, transforming growth factor-beta (TGF- $\beta$ ), fibroblast growth factor (FGF), platelet-derived growth factor (PDGF), and insulin-like growth factor-1 (IGF-1)<sup>29,30</sup>.

An active osteoblast is cuboid in shape and lines up on the bone surface with high secretory capacity when bone formation is proceeding<sup>30</sup>. Osteoblasts are responsible for the production and secretion of the organic matrix collagen type 1 and non-collagenous proteins, including proteoglycans (e.g., aggrecan), glycoproteins (e.g., osteonectin, bone sialoprotein, alkaline phosphatase (ALP)), and gamma-carboxylated protein (osteocalcin/Gla-

OCN)<sup>16,19,23,30</sup>. Osteoblasts are also involved in the subsequent mineralisation process<sup>23,26,27</sup>.

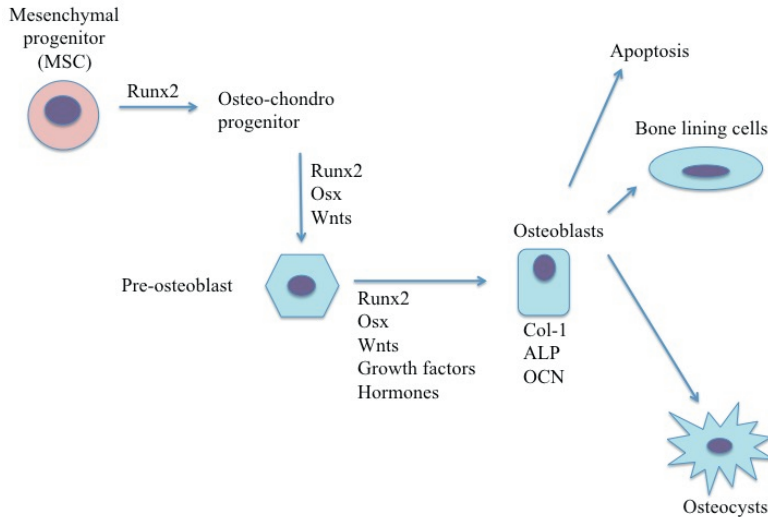


*Figure 2. Schematic illustration of the recruitment and differentiation of MSC to mature osteoblasts, a process that is regulated by many signalling molecules, including the transcription factors Runx2 and Osterix. In due course, the osteoblasts undergo either apoptosis or further development into bone-lining cells or osteocytes.*

## Osteocytes

Eventually, osteoblasts will develop into different forms, including apoptotic cells, metabolically low-activity bone-lining cells or entrapped dendritic osteocytes. The osteocytes are proposed to undergo numerous differentiation stages: Osteoid-osteocyte, pre-osteocyte, young osteocyte, and mature osteocyte. These cells are long-lived and represent the majority (90%–95%) of the bone cells in the adult skeleton<sup>27,30</sup>.

The mature osteocytes have developed cytoplasmic processes that are in contact with the adjacent osteocytes through gap junctions (allowing cell-cell interactions). They also communicate with other bone cells on the bone surface by small signalling molecules transported via canaliculi<sup>19</sup>. Osteocytes are believed to have a bone remodelling-regulatory function. When microfractures occur in the bone, caused by, for example, fatigue, osteocytes are believed to signal the need for remodelling. However, they are also proposed to secrete sclerostin, which decreases bone formation by inhibiting the ‘Wnt/

$\beta$ -catenin' signalling pathway in osteoblasts<sup>29,31</sup>. Moreover, osteoblasts and osteocytes are believed to produce matrix metalloproteinases (MMPs), which is involved in the degradation of collagen during bone resorption<sup>30</sup>.

## **Osteoclasts**

Osteoblasts produce both macrophage colony-stimulating factor (M-CSF) and receptor activator of NF- $\kappa$ B ligand (RANKL), which are cytokines that are necessary for the recruitment and activation of osteoclasts. The RANKL/RANK interaction mediates further the expression of additional osteoclast-specific genes for such as TRAP (tartrate-resistant acid phosphatase) and cathepsin K<sup>19,32</sup>. Osteoblasts also produce osteoprotegerin (OPG), which is a soluble decoy receptor for RANKL and that inhibit osteoclastogenesis. Thus, osteoclast recruitment, differentiation, and activity are dependent upon osteoblast/osteocyte signalling as well as cytokines and growth factors<sup>23,33,34</sup>.

After recruitment and activation, osteoclast precursors will fuse into large multinucleated osteoclasts. They are responsible for bone resorption in the bone remodelling process, bone healing, as well as during pathological conditions<sup>33</sup>. Osteoclasts anchor to the bone surface by integrins, which bind to among others, osteopontin in the bone matrix. After anchorage, the cell polarise, forming different membrane domains creating a “sealed zone”, within which the ruffled border is located and resorption can proceed. Osteoclasts express, furthermore, Tc1rg1, which encodes proton ( $H^+$ ) pump sub-unit that participates in decreasing the pH level. In the sealed resorption zone, the lower pH dissolves the mineral crystals and the proteolytic enzymes (e.g., cathepsin K) degrade the remaining organic compartment. The degraded products are endocytosed across the ruffle border and transported to the functional secretory domain in the cell membrane<sup>16,19,32</sup>.

### **1.2.4 Bone formation**

The mechanism of bone formation encompasses the production of osteoid matrix by osteoblasts, followed by the deposition of hydroxyapatite crystals. Collagen type I fibres, which represent 90% of the proteins in bone, are secreted in an organised manner by osteoblasts. In addition, non-collagenous proteins, which represent the remaining 10% of proteins, are produced and incorporated into the collagen matrix. The subsequent mineralisation process involves the nucleation and growth of hydroxyapatite crystals. The nucleation and deposition of hydroxyapatite crystals occurs adjacent to the collagen fibrils, where the concentrations of calcium and phosphate ions are

increased. It has been suggested that crystal deposition also occurs in osteoblast-derived matrix vesicles, which subsequently break and expose the crystals to the extracellular matrix<sup>16,35,36</sup>.

There are two different models of bone formation, which operate in embryonic development, as well as fracture healing: Intra-membranous and endochondral ossification. Intra-membranous bone formation starts as “ossification centres” composed of MSC and pre-osteoblasts in the fibrous connective tissue, which after differentiation initiate bone formation. In endochondral bone formation, the initial formation of hyaline cartilage creates the patterns used for bone construction. Intra-membranous bone formation is responsible for most of the bones in the skull and clavicles, usually flat bones, whereas endochondral bone formation is responsible for all the long bones<sup>17,19</sup>.

The anatomy of skeleton formation is determined by the genome. However, modelling and remodelling of bone are further dependent on systemic and local factors<sup>16,23,37,38</sup>.

## 1.2.5 Bone healing

Upon bone trauma, a haematoma is created initially, which controls blood loss and activates different molecular cascades. The haematoma consists mainly of aggregated platelets, polymerized fibrin molecules, growth factors, and bone marrow cells. The innate (non-specific) immune system activates and dominates the subsequent events, even if the adaptive (specific) immune system contributes. The coagulation cascade, the complement system, and cytokine release act as the “first line of defence” during cellular injuries. This process including increased permeability of the blood vessels, results in *dolor, calor, rubor, tumor et functio laesa* (pain, heat, redness, swelling and loss of function)<sup>15,39-41</sup>. The complement system plays an important role in the inflammatory process, through the actions of opsonin (phagocytosis enhancer) and anaphylatoxins, and also in the bone-regenerative process. Both C3 and C5 anaphylatoxin receptors are up-regulated during osteogenic differentiation<sup>42,43</sup>. Resident cells in the tissue, injured cells as well as platelets, release crucial pro-inflammatory cytokines, such as tumour necrosis factor- $\alpha$  (TNF- $\alpha$ ), interleukin (IL)-6 and IL-1 $\beta$ <sup>34,39</sup>. In rats, the expression levels of these early pro-inflammatory cytokines peak during the first 24 hours following injury, and rapidly decrease to almost undetectable values after 3 days<sup>34,39,44</sup>. It is further suggested that osteoclast regulatory cytokines (OPG, RANKL, M-CSF) are highly induced within the first 24h after trauma<sup>34</sup>. The cytokines and growth factors have multiple functions,

including the chemoattraction of haematopoietic cells (polymorphonuclear leukocytes, monocyte/macrophages) and MSC to the site of injury, the regulation of osteoclast function, and the initiation of angiogenesis. In addition, mast cell degranulation and histamine release recruits further phagocytes<sup>41</sup>.

The inflammatory response is regulated so as to protect the body against excessive tissue damage, and anti-inflammatory cytokines, such as IL-10, are released from regulatory T cells and other cell types to control the inflammatory responses. Furthermore, the MSC are stimulated to proliferate and differentiate to osteoblastic or chondroblastic lineages. Osteoblasts have been detected on titanium implant surfaces already after 1 day. After the formation of woven bone, the remodelling process is essential for replacing it with more organised bone<sup>15,23,32,40</sup>.

Bone is a tissue with the capacity to heal without forming a fibrous scar. Bone healing is dependent of a variety of cell types, molecular mediators and overlapping biological events. The biological mechanism leading to osseointegration is usually described as intra-membranous healing, while the mechanism of fracture healing is described primarily as endochondral healing. However, the healing mechanism is not only dependent of the therapy, but also the healing conditions. Thus, primary stability of implants and reduction of the fracture gaps and rigid fixation of fracture fragments, are crucial for the bone healing. Furthermore, if the fracture gap is reduced optimally, and minimum movement is allowed, as in direct bone healing, the fracture will heal in an intra-membranous fashion. While mobility and suppressed blood supply favour chondrogenesis, as in indirect bone healing. However, intra-membranous and endochondral bone formation may also take place in parallel<sup>15,39,40,45,46</sup>.

## **1.2.6 Bone remodelling**

The bone remodelling process, which is active throughout life, is necessary to maintain tissue strength and flexibility, through the replacement of old fragile bone with new bone. An equal amount of resorbed bone is replaced when the bone remodelling is balanced<sup>20,23</sup>. Approximately 10% of the bone mass will be replaced by new bone each year, even though the rate of remodelling decreases with age. The rate of bone remodelling is higher for trabecular bone than for compact bone, which explains why pathological conditions that affect the remodelling process are detectable earlier in trabecular bone. The remodelling is controlled by both local (e.g., autocrine and paracrine cytokines, and growth factors) and systemic endocrine factors

(e.g., glucocorticoids, oestrogen, and insulin), as well as by mechanical pressure<sup>16,17,19,20,22,37</sup>.

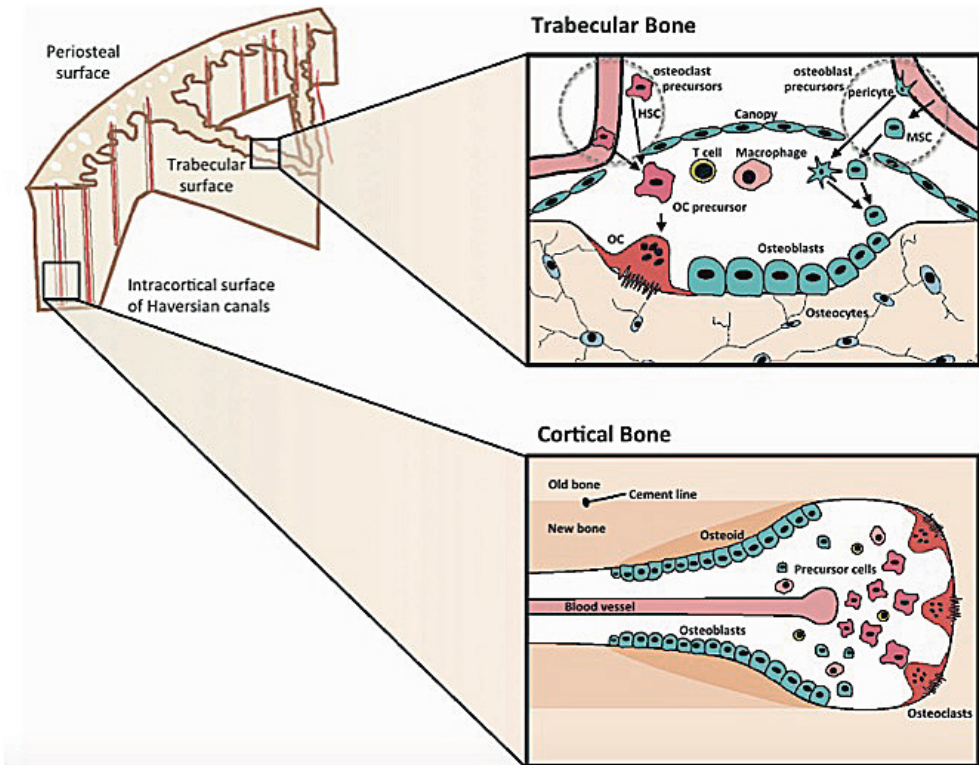


Figure 3. Schematic illustration of remodelling of: trabecular bone with bone cells lining the trabeculae surface (upper panel) and within cortical bone or Haversian canals (lower panel). T-cells, macrophages and precursors of osteoclasts and osteoblasts are recruited from bone marrow or blood. Reprinted with permission. Source;<sup>20</sup>. Copyright 2017 Creative Commons Attribution-Noncommercial-No Derivate Works 3.0 United States License. <https://creativecommons.org/licenses/by-nc-nd/3.0/us/>

Bone remodelling can be divided into five stages: Activation; resorption; reversal; formation; and termination. After an initiating remodelling signal, activation continuous with degradation of the non-mineralised osteoid on the bone surface by collagenases from the bone-lining cells and matrix metalloproteinases, produced by the osteoblasts/osteocytes. This process exposes RGD (Arg-Gly-Asp)-binding sites in the bone matrix proteins where the osteoclasts can anchor to the bone surface and subsequently resorb bone. The resorption stage concludes with the osteoclasts undergoing apoptosis or

it may divide into monocytes<sup>16,23,32</sup>. In the reversal stage, mononuclear cells of unidentified lineage remove the collagen remaining on the resorbed surface and form osteopontin-rich surfaces along the resorption track, thereby enabling osteoblast attachment and the deposition of osteoid matrix. When new bone is formed, the remodelling phase ends.

This interaction of bone cells, also called bone multicellular unites (BMU), can be described in terms of creating temporary anatomical structures<sup>20</sup>. Other cells that are present during the remodelling process are among others T-cells and resident macrophages (or Ostemacs)<sup>23</sup>. While the initiation of remodelling is not fully understood, it can be signalled by mechanical, hormonal or pro-inflammatory stimuli. Although the termination signals remain unknown, it has been suggested that osteoblast-inhibiting signalling via sclerostin plays a role<sup>16,20,23,30,32</sup>. If the balance between bone resorption and bone formation, i.e., the remodelling process is disturbed, pathological conditions resulting from either osteolysis or osteosclerosis appear<sup>18,37,38</sup>.

### **1.2.7 Pathological bone remodelling**

Pathological bone remodelling is a process through which the balance between bone formation and bone resorption is disrupted. Pathological bone remodelling occurs in several conditions, such as periodontitis, peri-implantitis, loosening of acetabular cup implants, osteoarthritis in joints, intra-osseous bone cysts and tumours, as well as bone metastasis. The most common condition with pathological remodelling is osteoporosis<sup>18,37</sup>.

#### **Osteoporosis**

While the pathogenesis of osteoporosis is complex and multi-factorial, it is essentially the creation of an imbalance between the osteoblast and osteoclast activities, leading to an increase in bone resorption relative to bone formation<sup>17,18,37</sup>. The condition can be primarily caused by oestrogen deficiency and ageing or secondarily caused by among others, endocrine conditions, alcohol abuse, anorexia, medication or bodily immobilisation. In females, primary osteoporosis pre-dominates owing to the biology of menopause. However, in men the proportion of those who suffer from secondary osteoporosis are larger. Osteoporosis is associated with decreased thickness of the trabecular bone, increased trabecular space, and loss of trabecular plates, leading to a progressive reduction in bone mineral density (BMD), decreased mechanical strength, and pre-disposition to fractures<sup>17,18,47,48</sup>. The  $\alpha$ -form of the oestrogen receptor (ER $\alpha$ ) has been proposed as playing a crucial role in bone turn-over. However, oestrogen

deficiency, in both females and males, is one of the major causes of osteoporosis in the adult population. The consequences of oestrogen deficiency include decreased production of OPG, increased production of cytokines, and decreased secretion of growth factors. Deficiencies of calcium and vitamin D (Calcitriol), as in secondary hyperparathyroidism, are additional mechanisms underlying the imbalance of remodelling in osteoporosis. Furthermore, ageing itself affects bone remodelling due to, for example, impaired mineralisation, aberrant periosteal responses to trabecular bone loss, and increased adipogenesis<sup>18,27,33,37,49</sup>.

## **Diabetes mellitus**

Diabetes mellitus (DM) is another condition associated with secondary pathological remodelling of bones. Insulinopenia (e.g., diabetes mellitus type I) is associated with decreased BMD, an increased risk of osteoporosis, and fragility fractures<sup>50,51</sup>. In animal models, this condition is associated with abnormal bone formation, altered bone micro-architecture, and affected bone healing which can be normalised through systemic treatment with insulin<sup>52,53</sup>. In clinical trials, the low BMD of diabetic patients has been associated with reduced mean levels of plasma IGF-1, ALP, and OCN<sup>54</sup>. In contrast to osteoporosis, which is considered a disease of the aging population, bone loss linked to DM type I occurs at a very young age, in that the BMD may be affected already at the time of diagnosis. However, the metabolic consequences of the disease over time have been suggested to be as important as the genetic pre-disposition<sup>50,51</sup>.

The pathogenetic profiles of DM types I and II differ in that insulin resistance, rather than the lack of insulin production, causes DM type II. Furthermore, DM type II predominantly affects the adult population. The studies in the literature are controversial regarding the potential linkages between BMD and fracture risk and insulin-resistant diabetes<sup>52</sup>. In a mice model of DM type II, Kawashima *et al.* demonstrated a decrease in bone volume, even though the BMD was not affected; this resulted in slender bones of decreased strength<sup>55</sup>. In clinical trials, DM type II has not always been associated with decreased BMD, but more often has been associated with normal or even increased BMD. However, both diabetic populations have shown associations with a higher risk of bone fractures and impaired fracture healing<sup>56</sup>. Hyperglycaemia, advanced glycation end-products (AGEs), reactive oxygen species (ROS), and prolonged inflammation, with consequent increased osteoclast activity, have all been proposed as factors that influence bone quality<sup>51,52,56,57</sup>. Visual impairment and peripheral

neuropathy, also contribute to a higher risk of falling for patients with DM type II, and this is pertinent to the increased risk of fracture<sup>52</sup>, despite a potential increased BMD. It is further suggested that oestrogen plays a crucial role in insulin-glucose homeostasis<sup>58</sup>, and ER $\alpha$ -knockout mice develop insulin resistance and are associated with increased body weight and abnormal glucose homeostasis<sup>58,59</sup>.

70,000 osteoporosis-related fractures occur in Sweden<sup>60</sup> annually. In Europe, the highest age-adjusted hip fracture incidences were found in women in Denmark and Sweden (574 and 539/100,000 respectively). The majority of the patients, who will require revision surgery because of post surgery complications, will result in temporary or permanent immobilisation and consequently significant costs for the society<sup>11,48,61</sup>. Both primary and secondary osteoporosis have impact on osseointegration and fracture healing<sup>62,63</sup>. In animal models, osteoporosis has been associated with decreased primary stability of the implant and decreased bone formation. In clinical trials, however, the outcomes for osteoporotic and healthy patients were not different, in terms of either implant stability or fracture healing<sup>40,64-66</sup>. It remains unclear as to whether these clinical outcomes are due to a modified surgical technique, compensating for the poorer bone quality or the difficulty associated with performing comparable clinical trials with acceptable quality<sup>64</sup>. In contrast, DM has been associated with impaired and delayed fracture healing, although not with increased failure rates for titanium implants in clinical trials<sup>50-52,56,63</sup>.

### 1.3 Insulin

Insulin is a peptide hormone (5808 Da), comprising 51 amino acid residues in two polypeptide chains (A-chain and B-chain), linked by disulphide bonds. The amino acid sequence of insulin hormone is similar among vertebrates, suggesting that the amino acid chains are highly conserved. The hormone is produced by beta cells in the islets of Langerhans, located in the pancreas. Subsequently, insulin is stored in vesicles in the form of stable hexamers. Upon signalling, the insulin is secreted as monomers (the active form, which is less stable over time). The release of insulin is not continuous but instead oscillates, thereby avoiding the down-regulation of insulin receptors during prolonged exposure to higher concentration of insulin<sup>17,18,67</sup>. Numerous cells in the body, including osteoblasts and osteoclasts, express insulin receptors<sup>68-71</sup>. The insulin receptor is a trans-membrane receptor of the tyrosine kinase family. It consists of an  $\alpha$ - and a  $\beta$ -subunit, which upon

ligand binding dimerise with the adjacent  $\alpha$ - and  $\beta$ -subunits, which results in the auto-phosphorylation and activation of the insulin receptor substrate (IRS)<sup>72</sup>.

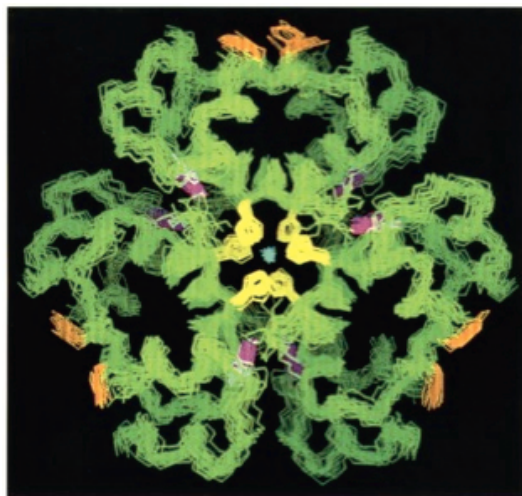


*Figure 4. The insulin hexamer is torus-shaped and the monomers are held together by zinc ions. The hexamer has a diameter of 50 Å and is 35 Å high<sup>73</sup>. Reprinted with permission. Source;<sup>74</sup>. Copyright 2017 American Chemical Society.*

The IRS further mediates the signal transduction via different pathways, such as those involving MAPK/ERK and PI3K/Akt<sup>75-77</sup>. The insulin receptors and IGF-1 receptors have similar structures, with insulin and IGF-1 capable of binding to each other's receptors to activate similar signalling pathways, albeit with lower affinities than when they bind to their own receptor<sup>17,78,79</sup>.

The importance of a rapid response to altered blood glucose levels coincides with the short plasma half-life of insulin (3–4 minutes)<sup>18</sup>. However, it is believed that the mean residence time of insulin until clearance is up to 70 minutes. Therefore, leaving the circulation is not equivalent to rapid destruction; it rather implies the effectiveness of its action. Furthermore, insulin-degrading enzyme (IDE), which builds a complex with the insulin molecule upon degradation, presumably exerts regulatory functions on steroid receptors and proteasomes. The clearance of insulin is mainly via hepatic uptake in the liver through internalisation into endosomes, where degradation takes place. The clearance of insulin has been suggested to play an important role in the development of pathological conditions, such as DM type II and obesity, in which hepatic clearance is reduced<sup>17,67</sup>. Currently,

biosynthetic human insulin is available for therapeutic usage, mainly for diabetes mellitus. To generate insulin derivatives with different properties, such as fast-acting and slow-acting, several analogues with minor changes to the amino acid sequence have been introduced<sup>18</sup>. Insulin is well known to aggregate in the interfaces and in solutions under specific conditions. The aggregation process is initially reversible and later irreversible, resulting in amyloid-like fibrils. These conformational changes may reduce its biological activity, which imposes limits on the storage of insulin<sup>80</sup>.

Insulin has effects on metabolism and other bodily functions, e.g., glucose homeostasis, vascular compliance, cognitive function and normal skeletal growth. Insulin regulates the blood glucose level in the body by signalling to the cells to activate some of the GLUT family receptors, which mediate intracellular uptake of glucose. Glycogenesis, which is the storage of glucose in the form of glycogen, is then started by hepatocytes and myocytes in the liver and muscles. Insulin is also known to increase amino acid uptake and the production of triglycerides<sup>17,18,67,81</sup>. Insulin is also a well-investigated hormone in cardiovascular disease, being identified as an anti-inflammatory factor. This hormone decreases the adhesion of leukocytes and platelets to the endothelium, and increases vasodilation<sup>82</sup>. Insulin administration also decreases the induction of TNF- $\alpha$  after induced acute myocardial infarcts, both *in vivo* and *in vitro*<sup>83</sup>. Dandona and co-workers have suggested that systemic treatment of obese non-diabetic patients, with insulin, has a significant acute anti-inflammatory effect<sup>84</sup>. In that study, the patients were injected with insulin for 4 hours and blood samples were collected. The level of intra-nuclear NF- $\kappa$ B in the mononuclear cells (MNC) was significantly reduced at 4 hours, the level of I $\kappa$ B (an inhibitor of NF- $\kappa$ B) in the MNC was significantly increased at 2 hours, and ROS generation by MNC was significantly decreased at 2 hours. Furthermore, alteration in both peripheral and CNS insulin action has been associated with memory impairment as in Alzheimer's disease. Insulin administration has been shown to enhance memory and performance in these patients<sup>85,86</sup>.

### **1.3.1 An osteoanabolic hormone**

Over the past decade, numerous investigations have elucidated the importance of insulin for normal bone growth<sup>68,69,72</sup>. Mice that lack insulin receptors on their osteoblasts have impaired post-natal acquisition of trabecular bone, as demonstrated by a decrease of >47% in the trabecular bone volume in relation to total volume. The affected trabecular bone was

associated with decreased osteoblast cell numbers and thickness, and increased trabecular spacing<sup>70</sup>. Furthermore, *in vitro* studies of insulin receptor-knockout osteoblasts from mice have shown decreased cell numbers, decreased cell differentiation, and increased sensitivity to apoptotic signalling<sup>69,70</sup>. Insulin has a potential role in regulating bone remodelling, while bone participates in the regulation of insulin secretion and cell sensitivity to insulin. It has been proposed that insulin mediates increased osteocalcin production and decreased OPG production. The altered OPG/RANKL ratio results in increased osteoclast activity, which contributes to acidification of the resorption lacuna. The low pH promotes the decarboxylation of osteocalcin. The under-carboxylated osteocalcin (Glu-OCN) has a reduced affinity for hydroxyapatite. This enables osteocalcin to enter the blood circulation, now as a hormone, and it promotes the insulin sensitivity of adipocytes and pancreatic insulin secretion<sup>70,87,88</sup>.

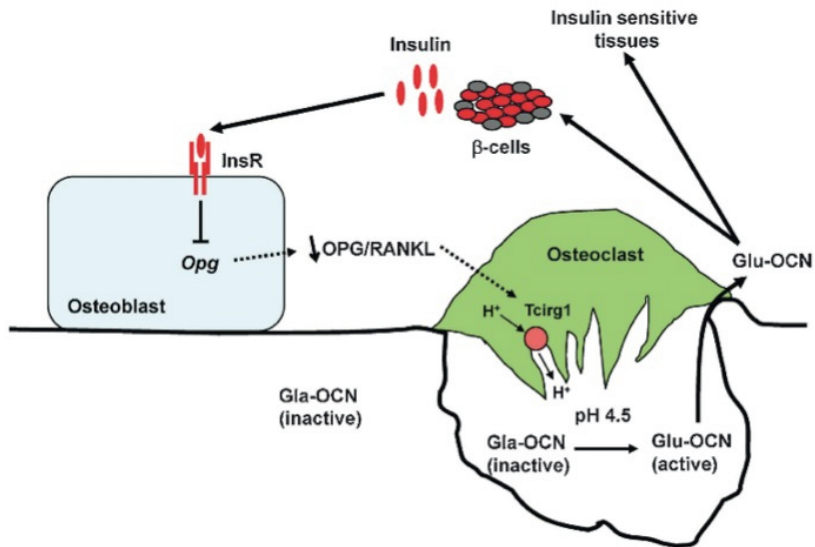


Figure 5. The insulin-receptor binding results in decreased OPG production. The decrease in the OPG/RANKL ratio results in increased expression of Tc1rg1 and increased osteoclastic activity. The acidic environment in the resorption pit promotes the under-carboxylation of osteocalcin. The under-carboxylated osteocalcin (Glu-OCN) enters the blood and increases adipocyte insulin sensitivity and insulin secretion from the pancreas. Reprinted with permission. Source,<sup>88</sup>. Copyright 2017 John Wiley and Sons.

In *in vitro* cell models, insulin treatment has been shown to induce osteoblast proliferation and differentiation, and the production of matrix proteins and

alkaline phosphatase<sup>69,75,89</sup>. Furthermore, except for the indirect stimulatory effect of osteoclasts, by decreasing OPG, contradictory inhibitory effects of insulin on osteoclastogenesis and osteoclastic bone resorption have been demonstrated *in vitro* and *in vivo*<sup>55,68,90</sup>. While other groups have found that insulin does not exert any stimulatory or inhibitory effect on osteoclasts either *in vitro* or *in vivo*<sup>91,92</sup>. Bosetti et al. analysed the effects of among others; insulin and IGF-I, on human primary osteoclast differentiation. Insulin did not increase either the differentiation or the resorption activity of the osteoclasts, in contrast to IGF-I (as demonstrated by calcium release and visually counting the bone-resorption lacunae on dentin slices)<sup>91</sup>.

The possibility of using insulin as an osteoinductive agent has attracted interest earlier. In 1931, Walter G. Stuck investigated whether “insulin could be used against delayed union of fractures”. He used a fibula fracture model in rabbits and injected insulin daily in the test group. He concluded that calcification of the callus seemed to be more advanced in the test group when examined microscopically, but not grossly detectable at 14 and 28 days. However, 5/15 rabbits in the test group died during the experiment due to side-effects of the systemic insulin treatment<sup>93</sup>. In 1996, Cornish and colleagues investigated the effects of insulin on bone *in vivo*, using daily injections for 5 days over the right hemicalvariae of adult mice. In the mice injected with insulin, they found significant increases in the osteoid area, osteoblast surface, and osteoblast number, as compared to the controls<sup>92</sup>. In 2005, Gandhi et al. presented the first attempt to improve bone healing (in a fracture model), using locally delivered insulin. However, this was conducted in a diabetic rat model and with palmitic acid as the carrier<sup>94</sup>. They demonstrated that local slow release of insulin normalised the fracture parameters, such as cell proliferation, mineralised tissue, and mechanical strength. Subsequent studies have been conducted to evaluate bone healing in rat fracture models<sup>95-97</sup> and lumbar spinal fusion<sup>14</sup>, in non-diabetic subjects. Paglia et al., showed increased expression levels of osteogenic markers (Col-1 and osteopontin), as well as increases in vascularity, mineralised tissue, and mechanical strength (4 weeks) in the insulin-treated group; however, the control group showed similar levels of mechanical strength after 6 weeks<sup>96</sup>. Dedania et al. showed histomorphometrically increased bone formation in the fracture gap (3mm) of rat femur. Furthermore, at 6 weeks, the insulin-treated group demonstrated bridging and union (n=7/7) of the defect, whereas the control group revealed no bony union (n=0/8). No control group without palmitic acid was included in this study, since the only control group consisted of palmitic acid carrier without

insulin<sup>95</sup>. Park et al. used a rat femur fracture model as well to demonstrate increased bone formation (radiographic evaluation) and increased mechanical strength after 4 weeks in the insulin-treated group, as compared to the control group, even though no increase in callus formation was evident after 2 weeks<sup>97</sup>. Koerner et al., discovered a significantly higher fusion rate after postero-lateral inter-transverse lumbar fusions from L4 to L5, when the rats were allografted with insulin-palmitic acid implants, combined with a bony autograft, as compared to blank allografts. Manual palpation after 8 weeks revealed fusions in 6 out of 10 rats in the test group, while the control group demonstrated fusion in only 1 out of 9 rats<sup>14</sup>.

Various delivery models have been used for local delivery of insulin, not only for evaluating bone healing but also wound healing in non-diabetic as well as diabetic systems. The models presented in the literature for local insulin delivery include: Direct injection of insulin into the site; the use of a palmitic acid carrier or calcium phosphate carrier and insulin incorporation into PLGA microspheres with and without fibrinogen gels<sup>14,95-100</sup>.

## 1.4 Titanium and osseointegration

Titanium is one of the most commonly used metals in medical applications, as it is biocompatible and has good physical properties. Biocompatibility, or the ability of a material to perform with an appropriate host response in a specific application, is determined partly by the rate of corrosion and the toxicity of the metal ions<sup>101,102</sup>. Upon exposure to air, a few-nanometres-thick oxide layer is produced on the titanium surface, mainly consisting of TiO<sub>2</sub><sup>103,104</sup>. This oxide surface passivates the metal, such that titanium implants exhibit strong resistance to corrosion in physiological environments<sup>101</sup>. Moreover, the titanium metal has a high strength-to-weight ratio, which means that it is a strong material with low weight. In the medical field, commercially pure (CP) titanium has historically been the most frequently used. CP titanium is graded on a scale of 1–4, where grade 1 is the softest and grade 4 is the strongest. The majority of dental implants used commercially today are CP titanium grade 4, however titanium alloys, in particular those of grade 5 (Ti6Al4V), are also used. The Ti6Al4V alloy is mainly used for orthopaedic purposes, but also as dental implants. Ti6Al4V has a higher resistance to fatigue and increased tensile strength, however, its capacity to osseointegrate has not been proven to outperform CP titanium of grade 4<sup>105,106</sup>.

Since the first titanium implant was placed in humans in 1965, the definition and underlying biological mechanism of osseointegration has been debated. Intensive research studies have attempted to clarify the biological mechanism of osseointegration. Osseointegration was first defined as a direct bone-to-implant contact without intervening fibrous tissue<sup>103</sup>, thus capable of load bearing of medical and dental devices. However, osseointegration can further be defined as the capacity of a material to mediate calcium and phosphate precipitation on the surface of that material, which will affect the subsequent bone response and may also ensure some mechanical stability earlier than the bone ingrowth. Thus, the formation of an apatite layer, derived from simulated body fluid, is a method used to predict the *in vivo* bone-bonding ability of a material. For instance, titanium is known to mediate apatite precipitation, whereas polyether ether ketone does not<sup>107</sup>. A recent study using advanced analytical tools has provided detailed information regarding the chemical composition of the bone-implant interface at the atomic level of resolution<sup>104</sup>. After the healing process in the bone, the titanium oxide layer showed incorporation of calcium ions, presumably derived from the living tissue. Adjacent to the oxide layer, a thin layer with an increased amount of calcium ions was observed, and this was followed by an amorphous calcium phosphate phase with subsequent dense bone showing sparse vascularisation. The surrounding bone did not show any measurable incorporation of titanium, indicating the passivity of the oxide layer. Thus, an inorganic interface was formed after replacement of the previous adsorbed protein layer<sup>104</sup>. Albrektsson and co-workers have further suggested that osseointegration is driven by the immunological response, which over time develops in to a sub-clinical chronic inflammation: “The foreign body equilibrium”, with osteosclerotic bone encapsulation of the implant<sup>108</sup>.

### **1.4.1 Titanium surface modification**

In 1981, Albrektsson and co-workers presented six parameters of importance for the establishment of osseointegration: The implant material; implant design; implant finish; status of the bone; surgical technique; and implant loading conditions<sup>103</sup>. The implant finish and the surface properties have been thoroughly investigated. Different techniques or combinations of techniques have been used to modify the surface properties so as to improve the bone responses<sup>109,110</sup>. Since osseointegration has been suggested to depend on biomechanical bonding (ingrowth of bone into irregularities of the titanium surface), the roughness of the implants was studied early. Wennerberg and co-workers presented guidelines as to how to analyse and present surface

topography in a standardised way. Furthermore, it has been suggested that a surface roughness level of about  $1.5 \mu\text{m S}_a$  is optimal for osseointegration<sup>111</sup>. This is rougher than the original Brånemark implant, which had a surface roughness of about  $0.5 \mu\text{m S}_a$ <sup>112,113</sup>. In order to modify surface roughness, blasting with small particles of different materials has been used<sup>109</sup>. Commercially available implants with this surface modification include TioBlast™ (Astra Tech), which is blasted with  $\text{TiO}_2$ <sup>114,115</sup>. Aside from changing the topography, efforts have been made to achieve chemical bonding between the titanium implant and the adjacent tissue. Materials that have the capacity to bond to living tissues are defined as “bioactive”. In the 1970s, the first bioactive material, Bio-glass hydroxyapatite, was described. However, this material was found to have poor mechanical properties and consequently deemed to be unsuitable for load-bearing and clinical applications. Therefore, a plasma-spraying technique was used to coat the titanium surfaces with hydroxyapatite (HA), which demonstrated an initially beneficial bone response, although subsequently the coating cracked and the implants failed. The experimental sol-gel coating represents an alternative approach to plasma spraying of HA. The sol-gel process involves the transition of a liquid phase to a solid phase. With further drying and heat treatment, the “gel” is converted into a dense ceramic, and thin films can be produced<sup>109</sup>. Alternative techniques have been presented to enhance bone formation. Incubating the implants in different acidic or alkaline solutions with or without subsequent heat treatment (alkali-heating), can be used to change the topography, incorporate different ions, and change the oxide properties. Osseotite™ (3i)<sup>115</sup> and Osseospeed™ (Dentsply implants) are commercially available implant systems that have surfaces that have been subjected to etching processes<sup>116</sup>. Incubating the implants in solutions with different electrolytes and concentrations, and applying a voltage (anodising), results in alterations to the surface chemistry, oxide thickness, surface roughness, and pore configurations<sup>109</sup>. TiUnite™ (Nobel Biocare) is a commercially available implant with an anodised /electrochemically oxidised surface<sup>117</sup>. One can also combine different process, as in the case of the SLA™ surface (Straumann), which is a surface that has been subjected to both blasting and etching<sup>115</sup>.

## 1.4.2 Protein surface modification

Immediately after implant insertion into the host tissue, complement factors, as well as coagulation factors will be activated and the titanium surface will be subjected to layering with adsorbed proteins in a provisional matrix. The

adsorbed layer consists of a large number of different serum proteins, such as C3, fibrinogen, albumin and globulins in different orientations and stages of denaturation<sup>118,119</sup>. Over time, the composition of this protein layer undergoes both conformational (denaturation) and orientational changes, with a continuous exchange of proteins with the environment<sup>120</sup>. The composition of the protein layer depends on the surface chemical properties, such as charge and hydrophilicity as well as the protein concentrations in the bodily fluids and is suggested to mediate further biological responses<sup>119 121</sup>.

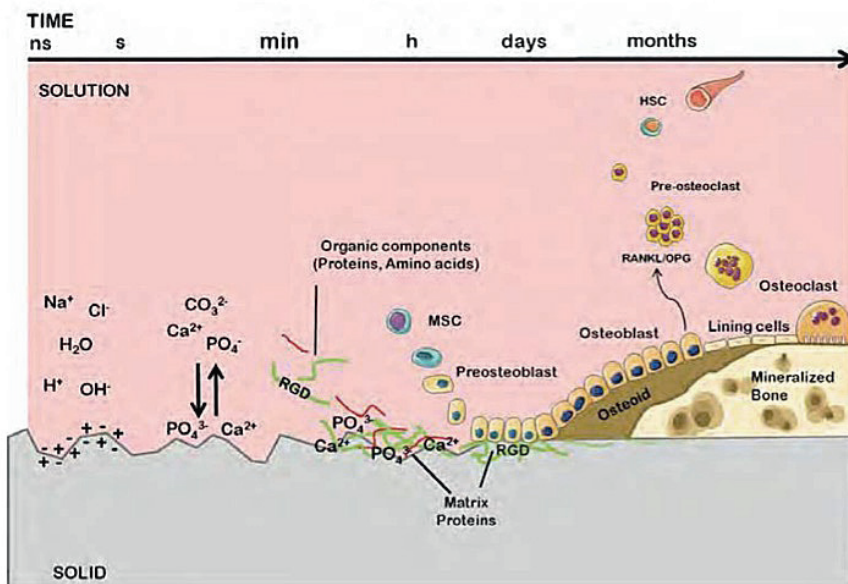


Figure 6. Schematic illustration of the time dependent biomaterial-tissue interactions at the interface, which will start immediately until equilibrium is reached and organic components are attached. These will attract pre-osteoblasts, whom after differentiation will continue the bone formation. Reprinted with permission from publisher/authors. Source,<sup>122</sup>.

The main goal in studying the interactions at the bone-implant interface is to understand how the surface structure and chemistry can be modified, so as to be able to control the cell responses that occur at the interface<sup>121</sup>. It is proposed that an artificial surface with precision immobilisation would control protein adsorption and subsequent biological responses.

To achieve this goal, titanium has been subjected to bonding (by immobilisation) of different molecules onto its surface, with the aim of creating a surface that can act as a delivery vehicle for proteins, peptides, and

drugs (e.g., BMPs, TGF- $\beta$ , IGF-I, RGD, bisphosphonates)<sup>123-126</sup>. BMP-2 and BMP-7 are approved by the Food and Drug Administration (FDA) for clinical use in specific conditions, such as open fractures of long bone and non-unions, however the growth factors are incorporated into a collagen matrix, and is released upon degradation<sup>127</sup>.

There are different methods to deliver molecules to the implant-tissue interface including: 1) Spontaneous adsorption of the molecule onto the surface before implantation or self-assembling monolayers (SAM); 2) incorporation of the molecule into a coating material-matrix; and 3) covalently or partially covalently immobilising the molecule to the implant surface. The latter requires pre-treatment of the surface to increase the number of available binding sites for the molecule. All three techniques have different disadvantages and advantages regarding the control of the number of molecules that are coated and the kinetics of release of the carried molecules.

In the present project, an immobilisation technique was used that is based on partial covalent binding of insulin to the titanium surface. This immobilisation technique has previously been used to immobilise proteins such as collagen, albumin, immunoglobulin G, fibrinogen, catalase, and bisphosphonates to different surfaces in multi-layers<sup>128-130</sup>. The technique is based on an initial silanisation step, followed by cross-linking of the protein to the silane *via* carboxyl activation and the formation of partial amide bonds<sup>131</sup>. This technique has not previously been used to immobilise the hormone insulin onto a surface.

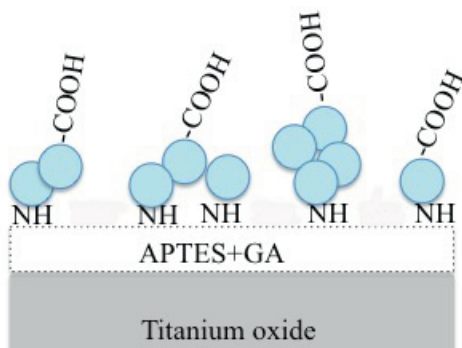


Figure 7. Schematic of the immobilised protein (e.g., insulin) layer on titanium-surface after silanisation (e.g., APTES + GA) and cross-linking of the protein.

## **2 OVERALL AIM**

The overall aim of this PhD thesis was to determine whether local administration of insulin, coated on a titanium surface has the potential to regenerate bone locally.

### **2.1 Specific aims**

- I. To investigate if local administration of insulin delivered from an implant surface enhances bone formation in non-diabetic rats.
- II. To analyse the release of insulin immobilised onto a titanium surface, over time and under different conditions, and to investigate the released insulin's biological activity in MG-63 osteoblast-like cell cultures.
- III. To characterise immobilised insulin behaviours on titanium surfaces, in biologically relevant cell culture medium, without and with the addition of serum proteins.
- IV. To evaluate the effects of local administration of insulin delivered from an implant surface on gene expression and bone formation in osteoporotic rats.

### 3 MATERIALS AND METHODS

Table 1. Overview of the performed experiments

Study	Study model		Evaluation of:	Evaluation time	Evaluation technique	Implants/ discs
<b>Pilot</b>	<i>In vitro</i>		Optimisation of the coating technique	-	Ellipsometry	Si-samples
			Characterisation of the titanium surface	-	SEM	Titanium grade 4, turned surface, mini-implants (2.1×2.0 mm), and Si-samples
<b>I</b>	<i>In vivo</i>	Healthy male rats, implant insertion in the tibia	Bone formation	4 weeks	Ellipsometry, Interferometry, Histomorphometry	Titanium grade 4, oxidised surface, mini-implants (2.0×5.0 mm)
<b>II</b>	<i>In vitro</i>	Incubation in cell culture medium	Insulin release from the titanium surface	1, 3, 9, 24, and 72 hours, and 1, 2, 3, 4 and 6 weeks	Ellipsometry, ECLIA	Titanium grade 4, turned or etched surface, discs (10.0×1.0 mm)
		MG-63 cell culture	Cell number	3 days	Ellipsometry, NR staining	Titanium grade 4, turned surface, discs (10.0×1.0 mm)
			Mineralisation process	Approximately 1 month	Ellipsometry, Alizarin Red staining	
<b>III</b>	<i>In vitro</i>	Incubation in cell culture medium	Chemical composition	1 and 10 days	Ellipsometry, XPS	Ti6Al4V alloy, turned surface, discs (8.0×1.0 mm)
<b>IV</b>	<i>In vivo</i>	Ovx rats, implant insertion in the tibia	Bone formation	1 day	Ellipsometry, qPCR	Titanium grade 4, turned surface, mini-implants (2.1×3.0 mm)
				3 weeks	Ellipsometry, Interferometry, Histomorphometry, qPCR, micro-CT, body weight, blood glucose	Titanium grade 4, turned surface, mini-implants (2.1×2.00 mm)
		Healthy and Ovx rats	General health	3 weeks	Micro-CT, body weight, blood glucose	-

## 3.1 Implant and sample preparation

### 3.1.1 Implants

Screw-shaped mini-implants (grade 4) and disc-shaped implants (grade 4 and grade 5) with different dimensions were used.

Surface modifications and qualities:

**Turned:** Titanium discs or mini-implants, CP grade 4, were used in Studies II and IV. The surface was machined in a turning process, giving a smooth surface<sup>103,112</sup>.

**Anodised:** The Ospol mini-implants used in Study I had calcium reinforced titanium-oxide surface (e.g., oxidised with the calcium ions present in the electrolyte) with micro-pores (1.0–1.5 mm in diameter). The 1–2-mm-thick outermost layer contained 11% calcium ions<sup>132</sup>.

**Etched:** Some of the discs used in Study II were subjected to an etching procedure, to modify the surface chemistry, by incubation for 2–3 minutes in 98% H<sub>2</sub>SO<sub>4</sub> plus 30% H<sub>2</sub>O<sub>2</sub> (volume ratio of 1:1).

**Titanium alloy:** In Study III, discs of the Ti6Al4V titanium alloy (grade 5) with turned surfaces were used.

### 3.1.2 Cleaning procedure

The implants were washed twice for 5 minutes each with 15 ml of Extran AP 15 (Merck, Darmstadt, Germany) plus 600 ml distilled water in an ultra-sonic water-bath set at 70°C. The implants were then rinsed three times with distilled water and twice with 70% ethanol (Solveco, Rosersberg, Sweden), and stored in ethanol over-night. The implants were dried on a sterile bench and sterilised in an autoclave (GE2609; Getinge, Sweden) at 134°C.

### 3.1.3 Immobilisation technique

The first step in the coating process was silanisation, whereby the ethoxyl group of (3-Aminopropyl)triethoxysilane (APTES; (Sigma-Aldrich, Steinheim, Germany) bound to the hydroxyl group of the titanium surface. Thereafter, an amine-reactive, homo-bifunctional (di-aldehyde) cross-linker, glutaraldehyde (GA; Sigma-Aldrich), was added. One of the aldehyde groups of GA bound to the terminal amino group of APTES and the second aldehyde group of GA bound to the amine group of insulin. Further cross-linking of insulin, *via* carboxyl activation (EDC-NHS), was achieved through the formation of partially amide bonds. Carboxyl activation was facilitated

by a carbodiimide, in the form of so-called zero-length cross-linkers. They are termed ‘zero-length’ because the carbodiimide facilitates the cross-linking without leaving a spacer molecule. Similar techniques have been used with other materials, such as silicon, stainless steel, collagen-based biomaterials and titanium<sup>128,130,133,134</sup>.

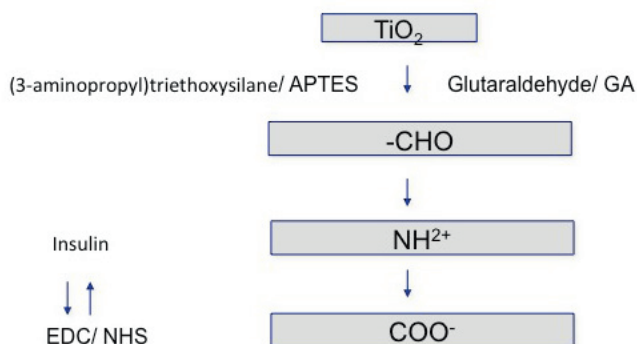


*Figure 8. The titanium oxide surface is first amino-functionalised with APTES. Coupling of insulin is then achieved via a di-aldehyde (GA). The aldehyde groups of glutaraldehyde (GA) will bind to the terminal amino group of the APTES and the amino group on the peptide/protein (in this case, insulin).*

The test implants and null ellipsometry reference Silicon (Si)-samples (1×1 cm) were subjected to the following insulin immobilisation process at room temperature<sup>133,134</sup>. First, the samples were incubated for 30 minutes in 1% APTES in xylene (VWR, Stockholm, Sweden), followed by rinsing with a series of 99% xylene, 70% ethanol, and distilled water, respectively. Thereafter, the samples were incubated for 30 minutes in 6% GA in phosphate-buffered saline (PBS; Sigma-Aldrich) (pH 9), and rinsed with PBS (pH 9). The recombinant, human insulin (in Study I: 95%, HPLC, semi-synthetic powder; Sigma-Aldrich and in Study II, III and IV: 10 mg/ml in 25 mM HEPES; Sigma-Aldrich) was diluted in PBS (pH 5.7) to a concentration of 1 mg/ml. The implants were incubated in the insulin solution for 15 minutes and then rinsed with PBS (pH 5.7). Between each layer of insulin, cross-linking and carboxyl group activation was achieved as mentioned above by incubating the implants in a PBS buffer (pH 5.7) that contained 0.2 M N-(3-Dimethylaminopropyl)-N'-ethylcarbodiimide (EDC; Sigma-Aldrich) and 0.05 M N-Hydroxysulfosuccinimide sodium salt (NHS; Sigma-Aldrich) for 15 minutes. The incubation in insulin solution and EDC-NHS was

repeated multiple times, depending on the experimental set-up. Thereafter, the discs were rinsed three times with PBS (pH 5.7) followed by distilled water, and finally dried with flowing nitrogen. As the EDC solution is unstable at room conditions, new solutions were prepared every 2.5 hours.

### **3.1.4 The insulin coating**

To evaluate the reproducibility of and the possibility to increase the thickness of the insulin coating, additional experiments were performed. Multiple changes were made to the above-mentioned coating process including:

1. After each incubation with insulin and EDC/NHS solution, additional drying with flowing nitrogen was performed.
2. Omitted the exchange of EDC/NHS solution every 2.5 hours.
3. Increased the incubation time from 15 minutes to 30 minutes.
4. Compared the insulin powder from Study I with the insulin solution from Study II, III and IV.
5. Replaced the washing step post-silanisation with flowing nitrogen.
6. Exchanged the insulin solution after 2.5 hours.
7. Instead of moving the samples with tweezers, in-between the incubation solutions, the solutions were exchanged and the samples were not moved.

To maintain a reference thickness of the insulin coating, ellipsometric measurements, as described below, were carried out at three different locations on five Si-samples after: a) the first washing step; b) incubation in APTES and GA; and c) the 1<sup>st</sup>, 5<sup>th</sup>, 6<sup>th</sup>, 7<sup>th</sup>, and 8<sup>th</sup> insulin incubations.

## **3.2 Surface analysis**

### **3.2.1 Interferometry**

To measure (in  $\mu\text{m}$ ) the surface topography, optical interferometry was used. In this method, the incident light is split into two beams, one that targets the sample and one that is on a reference plane. The technique measures the phase changes of the light reflected from the sample in relation to the reference plane. The measurements will be different at different locations depending on the roughness of the surface, thereby allowing a numerical description of the surface topography<sup>112</sup>.

Insulin-coated and non-coated implants were evaluated topographically in Studies I and IV. In Study II, the turned and etched non-coated discs were topographically evaluated using the MicroXam™ optical surface profilometer (ADE Phase Shift Inc., Tucson, AZ, USA). Discs and implants were measured over a  $200 \times 260\text{-mm}^2$  area, as described by Wennerberg et al.<sup>112</sup>. The implants were measured over the threaded area consisted of tops, valleys, and flanks. To measure the top and valley areas, the implants were placed in a horizontal position. To measure the flank areas, the implants were tilted. The raw data were processed with a form and tilt removal and extraction of the edges. A Gaussian filter ( $50 \times 50$  mm) was used to remove shape and waviness before the surface roughness was calculated. One height, one spatial, and one hybrid parameter were chosen to describe the surface topography numerically, as follows:

- Sa: the arithmetic mean height deviation from a mean plane.
- Sdr: the developed interfacial area ratio (i.e., the ratio of the increment of the interfacial area of a surface to the sampling area).
- Sds: the density of the summits (i.e., the number of summits of a unit sampling area).

### 3.2.2 Ellipsometry

Ellipsometry is an optical tool that is used for measurements of (at the sub-nanometre scale up to a few microns) thin films on a bulk material. It is based on a light source that is elliptically polarised by a generator and directed towards the sample. The light reflected after interaction with the sample, i.e., the change in polarisation, is detected and analysed.

The immobilised insulin film was quantified by null ellipsometry (HeNe laser-equipped Auto-El III ellipsometer; Rudolph Research Analytical, Hackettstown, NJ, USA) that was programmed for measurements in air. Since the titanium oxide has complex geometry, measurements were performed on reference Si-samples to establish a reference thickness of the film. These measurements were made at three to five different spots per sample, and the mean thickness of the bonded insulin was calculated after the thicknesses of the underlying APTES and GA layers were subtracted. The coat thickness was calculated according to the McCrackin evaluation algorithm<sup>135</sup> and converted to an approximate adsorbed amount per unit area using de Feijter's formula<sup>136</sup>. The assumed refractive index of insulin was  $n_f=1.465$ <sup>137</sup> and a 1-nm ellipsometric thickness of adsorbed molecules was equivalent to approximately  $0.12 \mu\text{g}/\text{cm}^2$ <sup>138</sup>.

### **3.2.3 Scanning electron microscopy**

SEM was used to image the surface morphology by scanning a focused electron beam over the surface. After interaction with the atoms in the sample, secondary electrons were collected, providing information on the surface morphology.

To visualise the thin insulin film on the surfaces of the titanium implants, SEM (Leo Ultra 55 FEG; Zeiss, Oberkochen, Germany) was applied to two control implants and two test implants. Additional imaging was performed on Si-samples non-coated, APTES–GA-coated, and insulin-coated. The instrument was equipped with a field emission electron gun (FEG) operated at 10 kV and images at a magnification up to  $\times 50,000$  were recorded.

### **3.2.4 X-ray photo-electron spectroscopy**

XPS was used to detect the chemical composition (in atomic %) of the outermost nanometres of the surface. The different functional groups, chemical bonding, and oxidation state of the sample could be recorded. Upon emitted photoelectrons a shift of the kinetic energy and peak intensity will be obtained.

In Study III, a Kratos Axis Ultra DLD X-ray photo-electron spectrometer with a monochromatic Al  $K_{\alpha}$  source operated at 150 W was used to detect the XPS spectra. A hybrid lens system with a magnetic lens and a charge neutralisation system were used. The binding energy (BE) scale was set at 285.0 eV and referenced to the C 1s line of aliphatic carbon. The Kratos software and CasaXPS packages were used for processing the spectra. Thereafter, curve-fitting of high-resolution C 1s and N 1s spectra was performed. Shirley background subtraction was carried out with spectral components corresponding to expected chemical states, two for the N 1s spectra and 3–4 for the C 1s spectra. The binding energy position and FWHM of the components were not fixed (however, they were not allowed to exceed 1.6–1.7 eV). The binding energy accuracy determination was 0.1 eV, and in atomic ratio: 8%–10 % rel.

## **3.3 *In vitro* study methods**

### **3.3.1 Electro-chemiluminescence immunoassay**

In Study II, the insulin concentrations in the cell culture medium samples (1 ml/sample) were analysed using an electrochemiluminescence immunoassay

(ECLIA, Cobas 8000 - e602 module) by the Clinical Chemical Laboratory at Umeå University Hospital, Umeå, Sweden.

ECLIA is based on an antigen sandwich technique. A biotinylated insulin-specific antibody captures the insulin in the culture medium, which then forms a complex with the ruthenium-labelled insulin-specific antibody. The complex generates a solid phase when treated with streptavidin-coated micro-particles attached to a magnetic electrode surface. Upon the application of a voltage, the electrode releases the chemiluminescence, which is measured with a photo-multiplier, revealing the insulin concentration in the sample.

### **3.3.2 Cells and cell culturing**

The human osteosarcoma cell line MG-63 (Sigma-Aldrich) was used in Study II. Compared to a human osteoblast, an attached MG-63 cell is smaller, its size does not differ with different cell densities, and it has a shorter doubling time<sup>139</sup>.

Depending on the experimental set-up, different numbers of cells were seeded in cell culture plates of different sizes. The cells were seeded in Eagle's Minimum Essential Medium (EMEM; Sigma-Aldrich) that was supplemented with 0.7 mM GlutaMAX, 1% benzyl-penicillin/ streptomycin, MEM non-essential amino acids (Sigma-Aldrich), and 10% FBS, in accordance to the supplier's recommendations. The cells were incubated in a humid atmosphere that contained 5% CO<sub>2</sub>, and the cells were split using 0.25% Trypsin-EDTA (Sigma-Aldrich).

### **3.3.3 Neutral Red uptake assay**

The Neutral Red (NR) uptake assay was used in Study II. This assay relies on the cell's ability to maintain different pH levels in different cell organelles. At neutral pH, the dye has no charge so it can enter the cell membrane. However, after entering the lysosome, which has a lower pH, the dye becomes charged and is captured inside the lysosome matrix in viable cells. Unbound substances are removed, so that only the intracellular NR can be extracted and measured by spectrophotometry as the optical density (OD) at 540 nm.

The cells were plated in 98-well plates and incubated overnight. Cell culture medium, without FBS and with or without the insulin, was added. The added insulin was from an insulin solution (10 mg/ml in 25 mM HEPES; Sigma-

Aldrich) diluted to different concentration or from insulin-coated discs incubated in the medium. After 3 days, the cell number was measured by the NR uptake assay, as described by *Repetto et al*<sup>140</sup> to evaluate the cell numbers in the different groups.

### **3.3.4 Mineralisation assay by Alizarin Red staining**

Alizarin Red staining was used to evaluate the formation of calcium-rich deposits of the cells in Study II. Calcium and Alizarin Red dye form a complex. The coloured mineral deposits can be visualised and quantitatively measured, since the dye can be extracted from the stained cell layer and measured spectrophotometrically.

At 100% cell confluency, the medium was exchanged every second day for 30–33 days. The mineralisation assay medium contained ascorbic acid and beta-glycerophosphate (Sigma-Aldrich) with and without insulin (from either an insulin solution, or released from insulin-coated titanium discs, as for the NR assay). The cells were then fixated in ice-cold 70% ethanol and washed with distilled water. Alizarin Red dye (ACROS Organics, NJ, USA) was added and the samples were incubated for 20 minutes at room temperature in the dark. The cultures were washed, dried, and visually inspected<sup>141</sup>. For quantification, the dye was extracted by incubating the culture plates at room temperature for 1 hour with 10% (w/v) cetylpyridinium chloride (CPC) (Sigma-Aldrich) in sodium phosphate ( $\text{Na}_3\text{PO}_4$ ) (Sigma-Aldrich), and the absorbance was measured at 540 nm using the Multiscan FC (Thermo Scientific)<sup>142</sup>.

## **3.4 *In vivo* study methods**

### **3.4.1 Animals**

The local Ethical Review Committee for Laboratory Animals (at Gothenburg University, Sweden) approved the animal experiments in Studies I and IV. The rats (Janvier Labs, Saint-Berthevin, France) were housed at the Laboratory of Experimental Biomedicine (EBM) at Gothenburg University, in accordance with institutional guidelines.

The Sprague Dawley rat, which is an outbred strain commonly used in medical research, was chosen for the present studies. These rats are characterised as a stable, heterogeneous stock. In Study I, healthy male rats (450 g in mean body weight) were used, and in Study IV, Ovx (470 g in

mean body weight) and healthy female rats (340 g in mean body weight) were used. Rats were kept at 2–3 per cage with access to water and food *ad libitum*. Each rat acted as its own control, except for the healthy rats in Study IV, which were compared to the Ovx rats. The Ovx rat model is approved by the Food and Drug Administration (FDA) as a pre-clinical model for studying potential interventions directed at affected bone metabolism in postmenopausal osteoporosis<sup>143</sup>. When the rats were 12 weeks of age, the provider performed an ovariectomy and delivered the animals to EBM. To ensure that the animals had developed osteoporosis, they were included in the study 5 weeks after the ovariectomy<sup>144</sup>.

### 3.4.2 Surgery

The surgical procedure was performed under aseptic conditions and the animals were treated under general anaesthesia: in Study I, with intraperitoneal injection of one part fentanyl–flunizone (0.2 mg/ml Hypnorm Vet; Janssen, Saunderton, England), two parts sterile water (Fresenius Kabi, Sweden), and one part midazolam (5 mg/ml Dormicum; Roche, Boulogne-Billancourt, France); and in Study IV, with isoflurane inhalation (Isoba Vet; Schering-Plough, Uxbridge, England). After weighing, the hind leg of each rat was cleaned with 0.5% chlorhexidine (Apoteksbolaget, Malmö, Sweden) and shaved. Identification of the animals was facilitated by pencil marks on the tails in Study I or with microchips injected subcutaneously between the scapulae (Agnthos AB, Lidingö, Sweden) in Study IV. Local anaesthetics (2% xylocaine-adrenaline; AstraZeneca, Sweden) were administered, followed by skin incision on the medial aspect of the proximal tibia metaphysis. Dissection of the muscles and periosteum was made until the tibia was exposed. The osteotomy was made using a rotary instrument (800 rpm) with a 1.4-mm and a 1.8-mm round drill under saline irrigation. The implants were installed unicortically into each tibia. The wound was closed in three layers with absorbable sutures (4/0 Vycril and 5/0 Monocryl; AstraZeneca). The animals received buprenorphine hydrochloride (0.03 mg/kg, Temgesic<sup>TM</sup>; Reckitt Coleman, Hull, England) at the surgery and on the first post-operative day. The animals were monitored in separate cages, until mobile. All the animals were thereafter checked daily. The animals were sacrificed with an injection of pentobarbital (100 mg/ml; Apoteksbolaget).

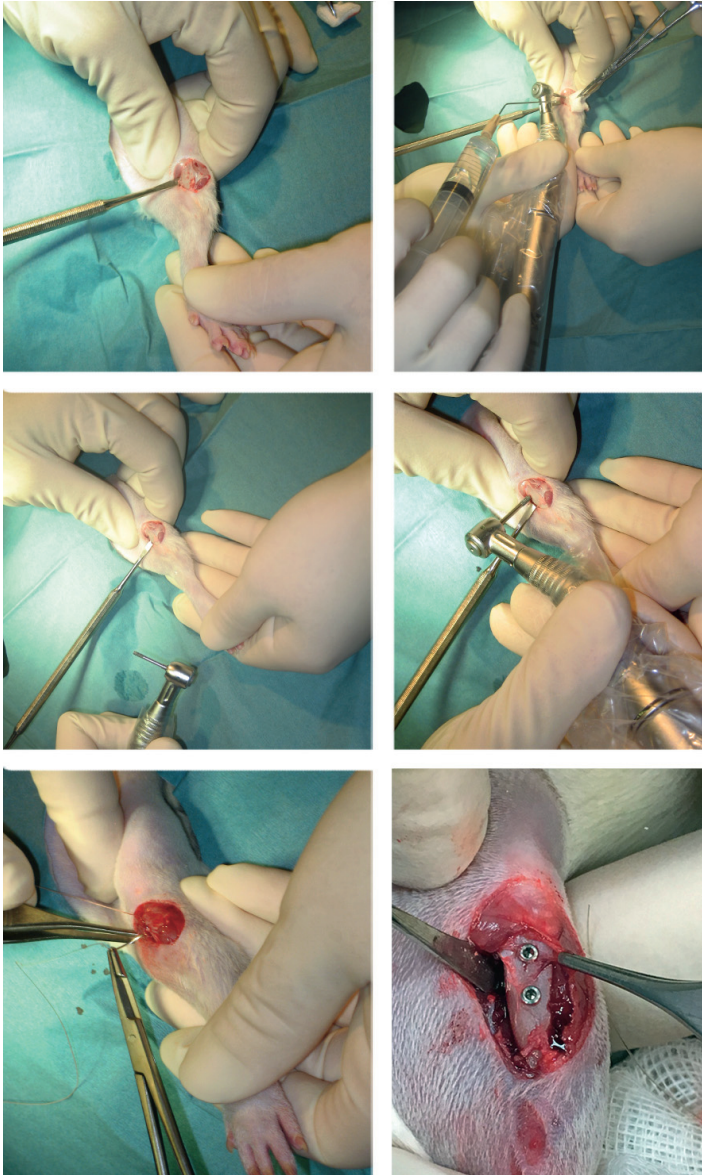


*Figure 9. The medial side of the tibia was exposed and the osteotomy site was prepared by drilling under saline irrigation. The test (insulin) and control implants were installed in different tibia in order to avoid any possible influence on each other. The wound was finally closed by suturing in 3 layers. Lower right panel: When two implants of the same group were installed in the same tibia, one was placed proximally and one distally. Only implants from the same group were installed adjacent to each other.*

The tibia was exposed once again. Implants for qPCR analysis were removed carefully with a hand-held screwdriver, and immediately placed in RNAlater (Qiagen GmbH, Hilden, Germany). After additional soft tissue removal, the implants with surrounding bone were harvested *en bloc* and fixed in 4% neutral-buffered formaldehyde.

### **3.4.3 Blood glucose measurement**

To evaluate potential systemic effects of the insulin-coated implants, the blood glucose levels were measured using a blood glucose device with test stripes (Accu-Chek Aviva; Apoteket, Sweden) in Study IV. The blood was collected using an injection needle from the lateral tail veins of healthy and Ovx rats with and without insulin-coated implants.

### **3.4.4 Micro-computer tomography**

The specimens (in Study IV) that consisted of a proximal implant and a distal empty osteotomy site were scanned and reconstructed into a three-dimensional (3D) structure with the SkyScan1176 micro-CT (Bruker, Antwerp, Belgium) using settings of 55 kV and 431  $\mu$ A for the scanning, and a 1.0-mm aluminium filter. The exposure time was set at 1500 ms, with X-ray projections at 0.47° intervals and scanning angular rotation of 360°, resulting in an 8.9- $\mu$ m pixel-sized image. Projection-reconstruction into 3D images was made using the NRECON software ver. 1.5.1 (Bruker), with a beam-hardening correction of 30%. The following software packages were used: Skyscan for scanning; NRecon for reconstruction; DataViewer for alignment; CTAn for data analysis; and CTVox and CTVol for volume rendering. For the implant-bone interface analysis, the dynamic range at reconstruction was set (at -0.03 to 0.3) so as to minimise the metal artefacts. To exclude further noise, analysis was also made of the empty osteotomy site, using a narrower dynamic range (-0.03 to 0.08), which increased the resolution between bone and soft tissue. The region of interest was chosen (cylindrical) with a diameter of 250 px. Analysis was made of the entire implant length, excluding the inner 200 px (representing the hole or the implant itself). Due to the bowed surface of the long bone, a rectangular region of interest in a vertical direction to the tibiae was chosen with dimensions of 250 px width, 400 px length, and 75 px depth, in order to analyse the periosteal compartment. Global thresholding was used for all the analyses of bone structures.

### 3.4.5 Histology and histomorphometry

All the fixated specimens of the implants and surrounding bone in Studies I and IV were dehydrated in a graded series of ethanol, infiltrated with plastic resin, and polymerised. The resin-embedded specimens were then cut with a diamond-coated band saw, along the long axis of the implant, ground to a thickness of 15–20  $\mu\text{m}$ , and stained with toluidine blue. Toluidine blue is a basic dye that binds to nucleic acids and appears as a blue colour under light microscopy.

Quantitative histomorphometry was carried out to measure the bone-to-implant contact (BIC) and the bone area (BA) within the threads. A light microscope with a 20 $\times$  magnification objective and a 10 $\times$  magnification eyepiece (Eclipse E600; Nikon, Tokyo, Japan) was used, together with the analytical software (TechnoOptik AB, Huddinge, Sweden).

### 3.4.6 Quantitative Real-Time PCR

Implant-adherent cells were analysed for gene expression after 1 day and 3 weeks in Study IV. TATAA Biocenter AB (Gothenburg, Sweden) performed the RNA extraction, reverse transcription, quantitative real-time PCR. A reference gene screening of 12 genes was initially set up to identify the optimal reference genes. The design of the different primer assays was performed in PrimerBlast and blasted to avoid unspecific products. To validate the assays, synthetic DNA fragments (gBlocks Gene Fragments; Integrated DNA Technologies, Coralville, IA, USA) were designed for all the assays. The assays had an amplicon length of 80–150 bp and an annealing temperature of approximately 60°C. The primers (Integrated DNA Technologies) were further validated by staining with an intercalating dye (SYBR Green; Sigma-Aldrich). The experiments were run on a LightCycler 480 platform (Roche) using TATAA SYBR Grandmaster mix (TATAA Biocenter AB).

The screws were replaced into safe-lock tubes that contained  $\beta$ -mercaptoethanol, RLT buffer and carrier RNA and homogenised in Tissuelyser (Qiagen). The extraction was carried out with the RNeasy Micro Kit including DNase treatment (Qiagen). The same volume of each sample was transferred to the reverse-transcription reaction. Samples were transcribed into cDNA using the TATAA GrandScript cDNA Synthesis kit (TATAA Biocenter AB).

Table 2. Assay list – 1 day

Abbreviation	Full gene name
<b>C3</b>	Complement component 3
<b>IL-1<math>\beta</math></b>	Interleukin-1 beta
<b>TNF- <math>\alpha</math></b>	Tumour necrosis factor- alfa
<b>ALP</b>	Alkaline phosphatase
<b>IL-10</b>	Interleukin-10
<b>Casp8</b>	Caspase 8
<b>Runx2</b>	Runt-related transcription factor 2
<b>CatK</b>	Cathepsin-K
<b>OC</b>	Osteocalcin/Bone gamma carboxylglutamate protein

Table 3. Assay list – 3 weeks

Abbreviation	Full gene name
<b>IGF-1</b>	Insulin-like growth factor 1
<b>COL-1</b>	Collagen type – 1
<b>OPG</b>	Osteoprotegerin
<b>WNT3a</b>	Wingless-type MMYV integration site family, member 3
<b>C3</b>	Complement component 3
<b>ALP</b>	Alkaline phosphatase
<b>OC</b>	Osteocalcin/Bone gamma carboxylglutamate protein

qPCR was performed with the TATAA SYBR Grandmaster Mix. All the assays; Chosen reference genes; (*YWHAZ* (tyrosine 3-monooxygenase/tryptophan 5-monooxygenase activation protein zeta), *HPRT1* (hypoxanthine-guanine phosphoribosyltransferase), and *TBP* (TATA box-binding protein)), genes of interest (Table 2 and 3), and a genomic

contamination control assay, were run in duplicate on the LC480 platform (Roche). A 3-step temperature program was applied, and detection was performed in the SYBR channel. The mean value for the replicates was calculated and normalised against the reference genes. In order to obtain the relative expression between samples, the lowest expression level was set at 1.

### **3.5 Statistical analysis**

The data were analysed using the SPSS Statistics software ver. 23 (IBM Corp., Armonk, NY, USA). Assumptions related to the normality and homogeneity of all the data were first analysed using the Shapiro–Wilk’s and Levene’s tests of homogeneity of variance, respectively. Depending on the result of the normality test, parametric or non-parametric analyses were chosen.

For the BIC, BA, micro-CT, and gene expression analyses, the Student’s paired *t*-test was used. A Chi-square test in a 2-way table was further used to assess significant differences in BIC <5% between the groups in Study IV. The Kruskal-Wallis one-way analysis of variance test and Mann-Whitney U-test (2 samples), followed by the Bonferroni *post hoc* test, were used for the NR and Alizarin Red results. For the insulin kinetics data, the Mann-Whitney U-test (2 samples) was used. The interferometric data were analysed both with the Student’s *t*-test (Study I) and the Mann-Whitney U-test (2-samples) (Study IV), depending on the different outcomes of the normality test. All the statistical tests were used to assess significant differences at  $p < 0.05$ .

### **3.6 Ethical approvals**

The animal experiments in Study I and IV were approved by the local Ethics Committee for Laboratory Animals at the University of Gothenburg (Dnr: 293-2009 and 186-2015, respectively).

## 4 RESULTS

### 4.1 Study I

Insulin was immobilised onto the titanium surface by APTES-GA silanisation and EDC-NHS, cross-linking to a reference thickness of 149 Å, as measured by null ellipsometry.

The optical interferometer measurements showed no changes to the surfaces topography upon insulin immobilisation, regarding parameters of Sa, Sds, and Sdr.

The animals were successfully treated and sacrificed 4 weeks post-implantation. Both the insulin-coated and non-coated samples showed integrated implants on visual inspection and osseointegrated implants under light microscopy. The histomorphometric analysis showed a significantly increased BA, when the rats were treated with the insulin-coated implant (35.1%), as compared to treatment with non-coated implants (25.2%). Even though the mean value of BIC was higher for the insulin-coated implants (67.0%), there was no significant difference compared to the non-coated implants (58.6%) (Figure 10).

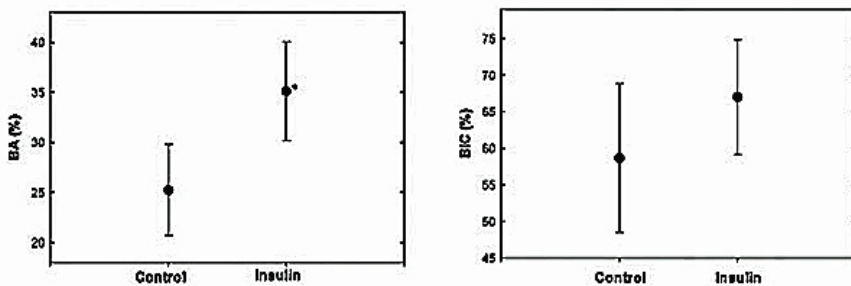


Figure 10. BA and BIC % for the control and insulin-coated titanium implant. The results are presented as mean  $\pm$  95% confidence interval. A statistically significant difference was found between the test and control groups regarding BA ( $p=0.005$ ).

### 4.2 Study II

The results showed insulin release from the insulin-coated titanium implants when they were incubated in cell culture medium with serum. After 1 hour of incubation, the mean of 35 nM in 1 ml medium or 25.9%  $\pm$  1.1% of the

initially immobilised insulin was released from the surface. The rate of release decreased rapidly and continued until the last evaluation time-point at 6 weeks. After 6 weeks,  $31.6\% \pm 1.4\%$  of the initially immobilised insulin had been released.

The release of insulin from the titanium implant was significantly increased as the insulin coating thickness increased, as well as when the surface was etched prior to insulin immobilisation. However, insulin release was significantly lower when the insulin-coated titanium implants were incubated in cell culture medium without serum proteins (mean of 3.4 nM insulin released), as compared to when they were incubated in cell culture medium supplemented with serum proteins (mean of 35.3 nM insulin released). Insulin release also decreased when the insulin-coated discs had been stored (dry and in dark) during 10 weeks before usage.

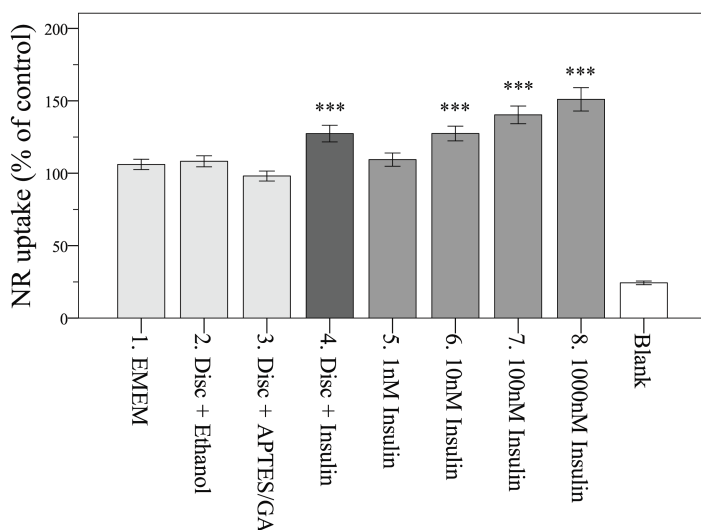


*Figure 11. Effects of insulin on cell number when cultured in medium with added insulin or insulin medium from incubated titanium discs. NR uptake in MG-63 cell line was used to evaluate the biological activity of the released immobilized insulin. Data are presented as % of control (EMEM), where mean is set to  $100\% \pm SEM$ . The figures are based on three identical experiments,  $n=24$ ,  $p<0.001$ . The cells were incubated in medium as described below: 1. EMEM 2. EMEM collected after incubation with non-insulin-coated disc washed with 70% ethanol. 3. EMEM collected after incubation with non-insulin-coated disc treated with APTES+GA. 4. EMEM collected from insulin-coated discs. 5–8. Insulin dilutions: 1 nM, 10 nM, 100 nM, 1000 nM.*

The released insulin retained its biological activity, as reflected in the significantly increased number of osteoblast-like cells after 72 hours ( $p < 0.001$ ) (Figure 11) and the significantly increased mineralisation capacity after 1 month ( $p < 0.001$ ) when treated with the released insulin.

### 4.3 Study III

The appearance of an intense nitrogen N 1s photo-electron line in the survey spectrum, as well as the similarities between the insulin-coated high-resolution spectra of C 1s and N 1s compared to insulin powder, confirmed the presence of a coated insulin layer. Insulin dominated the surface composition, even though a metallic component of the Ti was detectable, suggesting a non-homogeneous insulin layer. The non-coated titanium discs had other surface contaminants, such as F, N, Bi, Ba, and Pb. These findings were not replicated on the insulin-coated surface, which suggests that the coating resulted in the removal of the observed surface contaminants (Figure 12).

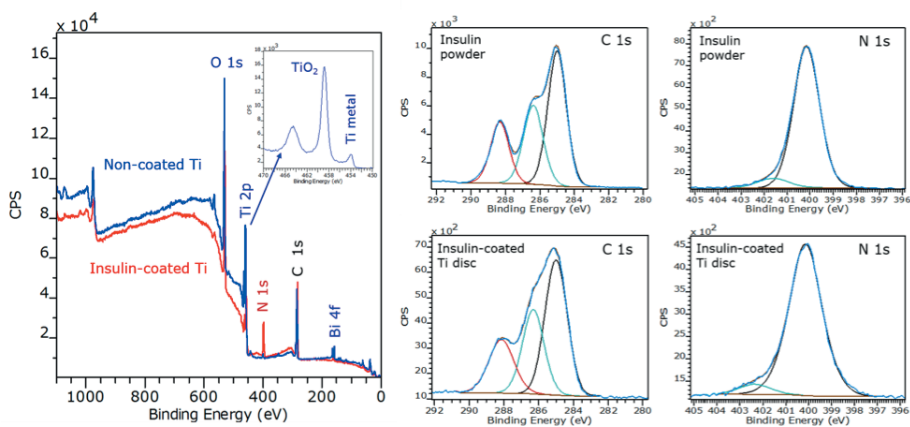


Figure 12. XPS spectra of non-coated (blue) and insulin-coated titanium (red) discs. Left: Survey spectra of non-coated and insulin-coated titanium. Upper right: Reference insulin powder C 1s and N 1s spectra. Lower right: C 1s and N 1s spectra of insulin-coated titanium.

The decreased atomic concentrations (at.%) of carbon and nitrogen, and increased titanium concentration seen after incubation in cell culture medium without FBS, indicated insulin release from the insulin-coated discs. The increased atomic concentration of carbon relative to nitrogen, together with the increase in intensity of the hydrocarbon component of the C 1s spectra

indicated a structural rearrangement of the insulin molecule that exposed hydrophobic parts of the molecules to the outside. The addition of FBS resulted in increased surface nitrogen, in spite of a small decrease in the atomic concentration of carbon. This indicated the adsorption of serum proteins on top of the non-released insulin coating. Furthermore, insulin-coated titanium discs incubated in both cell culture mediums did not have any carbonate adsorbed from the medium over time, which confirmed that the immobilised proteins remained relatively intact. However, structural rearrangements or conformational alterations within the protein layer appeared to occur, since the C 1s spectra revealed significant changes in the relative intensities of the spectral components. Finally, all the insulin-coated surfaces contained detectable levels of calcium and phosphate ions, despite the low concentrations of  $\text{CaCl}_2$  and  $\text{NaH}_2\text{PO}_4 \cdot 2\text{H}_2\text{O}$  in the cell culture media, which may play an important role in the enhancement of bone formation.

## 4.4 Study IV

The animals that received insulin-coated implants did not show any alterations of blood glucose levels or total body weight at start and 3 weeks post-implantation, compared to the controls.

A significant reduction in IL-1 $\beta$  gene transcription ( $p=0.019$ ) was detected for the insulin-treated samples, as compared to the controls, at 1 day post-implantation. 82% of the insulin-treated samples had the IL-1 $\beta$  gene transcription below the controls. However, no significant differences were detected for any of the other genes tested 1 day after implantation (TNF- $\alpha$ , C3, IL-10, Casp 8, ALP, OC, Runx2, Cat-K) and those tested at 3 weeks post-implantation (IGF-1, ALP, COL-1, OC, OPG, C3, WNT3a).

A significantly increased periosteal bone volume ( $p=0.029$ ) was detectable with micro-computer tomography, at 3 weeks post-implantation in the rats that received insulin-coated titanium implants, as compared to the controls (Figure 13).

The histomorphometric analysis revealed that only 17% of the 150 threads of the insulin-coated implants had a BIC value  $\leq 5\%$ , as compared to 31% for the control group. Thus, the numbers of threads with BIC values  $\leq 5\%$ , representing the worst outcome cases, were significantly lower in the insulin-coated implants than in the control implants (OR 2.18, 95% CI, 1.26–3.76;  $p=0.005$ ). The average BIC of the insulin-coated implants was 22.7%,

compared to 18.0% in the control group. No difference in bone area was found between the groups (30.3% and 30.5% for the insulin-coated and control groups, respectively).

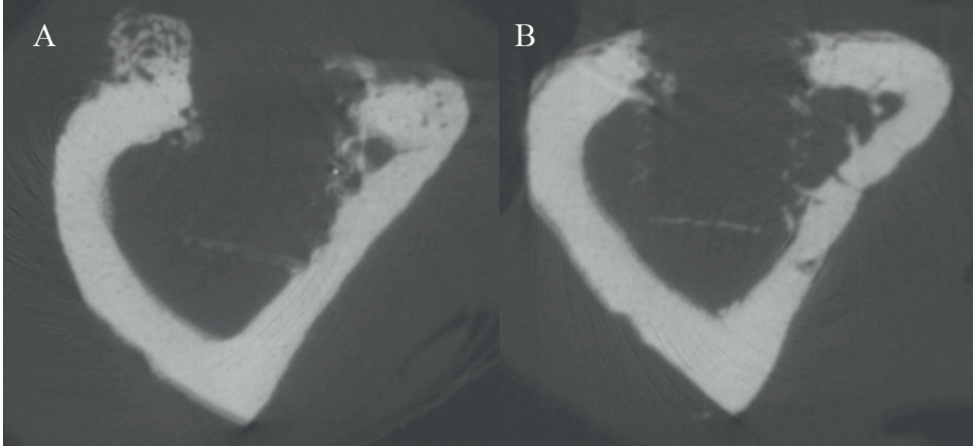


*Figure 13. Micro-computer images of the rat tibia after the removal of the titanium implants. Statistically more periosteal callus formation was found in the insulin-coated group (A) compared to the non-coated (B) ( $p=0.26$ ).*

## 4.5 Pilot study

Additionally, a pilot study was conducted in order to improve the insulin coating process.

In the pilot study, it was demonstrated that the changes made to the original immobilisation protocol (described in Material & Methods, 3.1.4) did not result in a thicker insulin coating (Table 4).

Furthermore, the number of insulin incubations did not correlate with the thickness of the insulin layer on the surface, since additional incubations resulted in increased and sometimes decreased insulin thickness (Figure 14).

The reproducibility of the immobilization technique was sub-optimal, since the final coating thickness across different immobilisation experiments, in these pilot series, differed from 25 Å to 55 Å (see control in table 4). It was therefore decided that a more reliable method to evaluate the amount of immobilised insulin was to use null ellipsometry for measuring the thickness of the layer, after each round of incubation with insulin.

*Table 4. Comparison of control and test (modified) methodologies for coating insulin onto titanium discs.*

<b>Modification of the original immobilisation process.</b>	<b>Control; thickness of coating (Å)</b>	<b>Test; thickness of coating (Å)</b>	<b>Outcome</b>
1. After each incubation with insulin and EDC/NHS solution, additional drying with flowing nitrogen was performed	51	52.3	Not significant
2. Omitted the exchange of EDC/NHS solution every 2.5 hours	41	40.5	Not significant
3. Increased the incubation time from 15 minutes to 30 minutes	25	30.4	Not significant
4. Compared the insulin powder from Study I with the insulin solution from Study II, III and IV	41	33.4	Not significant
5. Replaced the washing step post-silanisation with flowing nitrogen	48	23.2	Significant. The test group had decreased coating thickness
6. Exchanged the insulin solution after 2.5 hours	52	35.7	Significant. The test group had decreased coating thickness
7. Instead of moving the samples with tweezers, in-between the incubation solutions, the solutions were exchanged and the samples were not moved	55	21.9	Significant. The test group had decreased coating thickness

*\* Presented as mean, n = 5 and each Si-samples was measured at 3 different spots.*

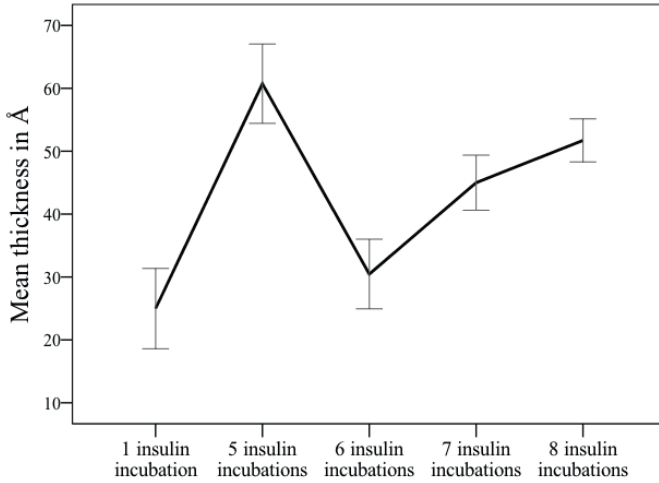


Figure 14. Thickness ( $\text{\AA}$ ) of the immobilised layer after 1, 5, 6, 7, and 8 incubations in insulin-solution. Values shown are mean  $\pm$  SEM,  $n=5$ , and each sample was measured on three spots.

The SEM images of the insulin-coated titanium discs revealed round-shaped structures scattered over the surface. These structures had different sizes, estimated at around 50 nm in diameter. The structures were not homogeneously distributed, but appeared in patches. However, these structures were visible on the Si-samples that only had been coated with APTES-GA, as well as on the insulin-coated samples (Figure 15). There was no significant difference in morphological appearance between the Ti and Si insulin-coated samples.

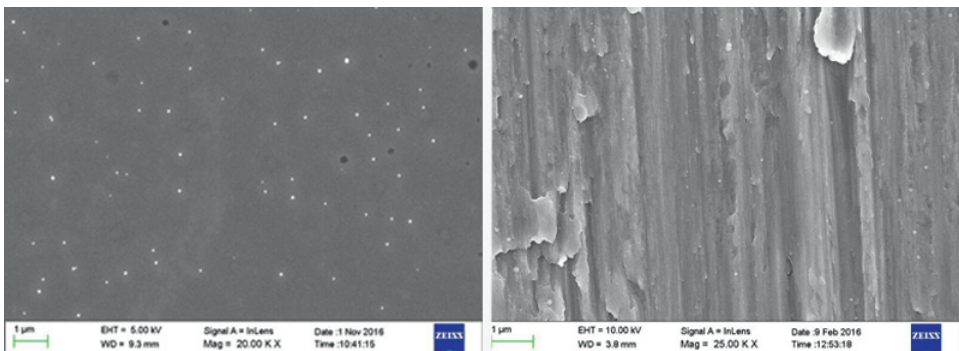


Figure 15. SEM image of Si-samples after incubation in APTES and GA and insulin-coated titanium implants, respectively.

## 5 DISCUSSION

In this thesis, the aim was to determine if insulin-coated titanium implants have the potential to enhance local bone formation. In summary, the results demonstrated that the insulin immobilised on the titanium surface was released with preserved biological activity and enhanced bone formation in healthy (bone area in the threads) and osteoporotic (periosteal callus formation) models. This means that insulin can be a possible agent for enhanced local bone formation. However, the currently used immobilisation technique has certain limitations, including problems with controlling the insulin concentration and storage.

In Study I, it was demonstrated that insulin-coated titanium implants enhanced the bone formation adjacent to the implant. Even though previous groups had aimed on local delivery of insulin to affect bone healing in non-diabetic subjects<sup>95-97</sup>, no one had previously used a coating model as a delivery system for insulin. In the clinical situation, titanium implants or fixation plates (i.e., potential insulin carrier), are expected to neither be degradable nor removed, therefore no additional intervention is needed.

In Study II, it was demonstrated that approximately one-third of the immobilised insulin was released in a burst-release manner after incubation in cell culture medium. Proteins such as insulin tend to be randomly folded when adsorbed or immobilised onto a biomaterial surface, i.e., the receptor-binding site may not always be visible<sup>126</sup>. Thus, the release of the protein is of interest, as are the time-dependent configurational changes that occur within the protein layer, as revealed in Study III, in order to facilitate receptor availability. Furthermore, insulin has been shown to decrease in uptake over time because of receptor down-regulation, which occurs mainly via internalisation<sup>69</sup>. Since the internalisation of the insulin receptors is a time-dependent process, an initial high concentration of insulin may be important. Thus, a high initial rate of protein release from the surface may be advantageous in the case of insulin. In Study II, significantly more insulin was released from the titanium surfaces when serum-enriched medium was used, as compared to serum-free medium. This correlates with the findings in Study III, suggesting the partial replacement of insulin by serum proteins, with insulin remaining as the major constituent at the surface. However,

despite this substitution, immobilised insulin stabilises the structures of all the proteins (insulin and additional adsorbed serum proteins).

Another finding was the incorporated calcium and phosphate ions in the protein layer after incubation in a cell culture medium, as described in Study III. Increased concentrations of calcium and phosphate ions are of importance for the mineralisation process and bone formation<sup>36</sup>. Furthermore, calcium-reinforced titanium implants have been shown to induce calcium phosphate precipitation at the implant surface<sup>132</sup>. If this ion incorporation is unique for the insulin-coated surface or a general mechanism for proteins coated to surfaces, needs further evaluation.

Glutaraldehyde (GA) has been used for chemical cross-linking of collagen matrixes to stabilise and increase their mechanical properties. GA has been shown to leave unreacted functional groups (aldehyde groups), which can result in cytotoxic reactions following the degradation of the collagen matrix<sup>128</sup>. However, in Study II, it is demonstrated that neither the silanisation nor the titanium surface *per se* has any effect on cell numbers *in vitro*. Furthermore, the results described in Study III indicate that protein immobilisation removes most of the normally observed contaminants on the titanium surface.

Since the MG-63 cells express insulin receptors and produce Col-1 and OCN, they provide a suitable model for studying the effect of insulin on osteoblastic function<sup>75,139</sup>. Analysing the responses in a cell line provides consistent and reproducible results. However, the results described in Study II need to be confirmed in primary human osteoblasts, in order to include inter-individual variations. Furthermore, the *in vitro* model is not always suitable for evaluating whole-body systemic effects. Insulin acts not only local on bone cells but also via endocrine signalling, resulting in increased insulin secretion and insulin sensitivity<sup>70,87,88</sup>.

Insulin treatment results in an increase in cell numbers and increased mineralisation process in MG-63 cells, as shown in Study II. The lack of insulin signalling in osteoblasts has been demonstrated to play a crucial role in bone formation in insulin receptor-knockout osteoblasts, *in vivo* and *in vitro*<sup>70,87</sup>. However, contradictory results have been reported for studies

involving the addition of insulin *in vitro* to osteoblasts that have insulin receptors; Yang et al. have shown increases in the mineralisation process, ALP activity, and secretion of Col-1, as well as increased numbers of MG-63 cells<sup>75</sup>; whereas Levy et al. showed a down regulation of ALP activity after incubating rat osteoblastic cells in insulin<sup>71</sup>. Zhang et al. have reported an increased mineralisation process, although they could not show increased numbers of primary calvarial osteoblasts<sup>77</sup>. This is in agreement with the results reported by Bosetti et al.<sup>91</sup>. Furthermore, Fulzele et al. have reported increased numbers of primary calvarial osteoblasts that lack IGF-1 receptors<sup>79</sup>. The heterogenous results may reflect that different experimental set-ups with different cell cultures can result in different outcomes.

Quantitative real-time PCR was used in Study IV to evaluate the early and late cellular responses to the insulin-treated samples. A previous *in vivo* study involving local delivery of insulin showed increased gene expression of osteopontin in the bone callus after 4 days, and increased *Col-1* gene expression after 7 days<sup>96</sup>. When analysing mice osteoblasts that lack insulin receptors, Fulzele et al. showed decreased levels of *Runx2* and *OCN* gene expression and increased *OPG* gene expression, as compared to controls<sup>70</sup>. However, Yang et al. reported down-regulation of *Runx2* expression and up-regulation of gene expression for *Osx* and *OCN* in MG-63 cells treated with insulin<sup>75</sup>. The increased expression of the *OCN* gene is in agreement with the report of Zhang et al., who showed an increase in *OCN* gene expression following the treatment of primary mice calvarial osteoblasts with insulin<sup>77</sup>. In Study IV, however, only one of the tested genes (*IL-1 $\beta$* ) showed a differential response compared to the control when treated with insulin, which might emphasise the difficulty related to determining the optimal sampling time for the quantitative real-time PCR.

In Study IV, decreased expression of the gene for *IL-1 $\beta$*  was noted for the insulin-treated samples, 1 day post-implantation. Insulin has been the subject of investigations of cardiovascular diseases with respect to its anti-inflammatory effect. The hormone has been shown to: Decrease the adhesion of leukocytes and platelets to endothelium; increase vasodilation; and decrease *TNF- $\alpha$*  expression both locally and systemically<sup>82</sup>. Dandona and co-workers have further shown that insulin treatment of obese, non-diabetic patients results in significantly decreased production of *NF- $\kappa$ B* by their mononuclear cells<sup>84</sup>. Inflammation at an early stage of the healing process is suggested to be of importance for bone healing mechanisms<sup>39,41</sup>. Anti-

inflammatory agents have previously been proven to affect the bone healing negatively<sup>145</sup>. However, an increased or prolonged inflammatory response may compromise the healing process. Furthermore, pathological conditions, such as oestrogen deficiency, diabetes mellitus, and periodontitis, are correlated with increased levels of pro-inflammatory mediators<sup>37,56,146,147</sup>.

In Study I, a significantly larger bone area was observed at the threads of the insulin-coated implants. This contrasts with Study IV, in which no significant differences in average bone area were observed between the groups. In Study I the reference insulin thickness was 149Å compared to 48Å in Study IV. Since normal bone metabolism is affected in ovariectomised rats, differences between the groups could be more difficult to discern, and a higher concentration of insulin might have been needed. In Study I, it is suggested that the significantly increased bone area seen for insulin-coated implants is a consequence of the released insulin stimulating the bone in the periphery. This suggested release of insulin is confirmed in Study II.

In accordance with the results obtained in Study I, no increase in the average BIC value was found in Study IV. However, significantly fewer threads with  $\leq 5\%$  BIC were seen after treatment with insulin. This may be interpreted as the most severe cases in osteoporotic rats being improved by locally delivered insulin. However the functional significance of having fewer threads with BIC  $\leq 5\%$ , if the overall BIC% is not significantly different, needs to be further evaluated.

The micro-CT evaluation described in Study IV provides new information regarding the significantly increased periosteal bone formation seen after implantation of the insulin-coated titanium implants. This finding may be of greater relevance for fracture healing than for osseointegration, as bridging of the fracture gap is dependent upon periosteal activity. Fracture healing has been suggested to occur in two stages: A primary callus response; and a secondary callus response. The first stage is characterised by subperiosteal new bone formation adjacent to the fracture, while the second stage is characterised by bridging of the fracture gap with an external callus<sup>46</sup>. A previous study<sup>95</sup> using a femur rat fracture model has shown increased endosteal bone formation following treatment with locally delivered insulin. However, in that study, an insulin-palmitic acid implant was used, which was allografted intramedullary, and therefore came in direct contact with the endosteum<sup>95</sup>. The enhanced periosteal bone formation observed in Study IV,

could also be a result of the coating detaching from the surface once implanted, contributing to a higher concentration of insulin at the periosteal site and consequently lower in the trabeculae compartment. The mechanical stability of the insulin coating has not been thoroughly investigated. However, if the coating has low mechanical strength, a surface with micropores, within which the insulin molecules are protected during implantation, might be favourable, as in Study I.

In Study II, a decrease of released insulin is demonstrated upon storage of the insulin-coated titanium discs. This is probably due to denaturation of the protein layer over time. As this has ramifications for the clinical usability, further studies are needed in order to solve these problems.

In study III it was demonstrated that the immobilisation of insulin onto a titanium surface resulted in a heterogeneously distributed insulin layer, as shown by the XPS analysis, which demonstrates that insulin dominates the coated surface, although the metallic component of the Ti 2p spectrum is also detectable. A non-homogenous surface was further visualised by SEM, showing a scattered distribution.

The thickness of the insulin layer has been used as a measure of the amount of surface-immobilised insulin, since it is shown in Study II that the thickness of the insulin layer corresponds to the amount of insulin released from the titanium surface. However, to receive a desirable insulin coating thickness or to reproduce a certain insulin thickness throughout the multiple coating occasions were difficult. In a previous study conducted by Tengvall et al., a gradual increase in the thickness of the layer of coating protein (IgG, fibrinogen, catalase, plasma proteins) on silicon was observed after each incubation with the coating agent, using the same immobilisation technique as in this study<sup>133</sup>. In this study, the insulin thickness, in some instances, decreased dramatically during the coating processes. The discrepancy between this study's results and those of the previous study<sup>133</sup>, cannot be attributed to the different surface materials used (silicon and titanium), as both surfaces were prepared and silanised according to a similar protocol. A factor that may be of importance is the quality of the immobilisation chemicals, in that EDC/NHS is susceptible to spontaneous degradation in aqueous solutions. In addition, an excessive concentration of EDC may result in protein degradation and detachment from the carrier surface<sup>148</sup>. Another likely explanation for the above-mentioned discrepancy may be that the

small protein-size insulin behaves differently than larger proteins (e.g., IgG, fibrinogen, and catalase), during immobilisation. However, to increase the amount of coated insulin, i.e., the coating thickness, and to prevent its removal upon implantation, the use of other carrier surfaces with different topographies (micro-pores) might be advantageous<sup>149</sup>.

The coating process used in Study IV significantly changed the surface topography, as compared to the control, even though the insulin-coated surface could still be regarded as a smooth surface. However, an altered surface topography might *per se* change the cell and bone responses<sup>110</sup>. In a review of the *in vitro* and *in vivo* models, it has been concluded that the properties of the implant surface (e.g., surface roughness) play crucial roles in the tissue responses that occur post-implantation<sup>150</sup>. In Study I, no significant change in the surface topography was detected after the immobilisation of insulin. The titanium surface in this study had a rougher surface with micro-pores, suggesting that the insulin molecules might have been protected within these pores.

In Study II, it is shown that osteoblast-like cells do not increase in number when incubated in cell culture medium that contains 1 nM insulin, as compared to incubation in the control medium. However, the cell numbers significantly increase when incubated in 10 nM, 100 nM, and 1000 nM of insulin. These findings indicate that insulin dose-dependently, increases cell numbers and is in agreement with other studies<sup>89</sup>. However, the difficulties with controlling the thickness of the insulin layer, represent a limitation to testing different insulin concentrations *in vivo*.

Locally delivered insulin has been studied in different non-diabetic models, not only to assess the possibility to improve the healing of bone fractures<sup>95-97</sup>, implant insertions<sup>100,151</sup>, and spinal fusions<sup>14</sup> but also to improve cutaneous wounds<sup>98</sup>. Insulin increases the migration of human keratinocytes, which suggests that it might promote wound healing<sup>98</sup>. The average blood vessel density within the sub-periosteal mineralised region (judged by manually counting the stained PECAM1-positive and VEGF-C-positive cells) showed a 75% increase after insulin treatment in a femur rat fracture model<sup>96</sup>. Alteration of the healing capacity of the cutis/mucosa and blood vessels might determine the outcome of fracture healing, grafting and osseointegration. Furthermore, enhanced bone formation, as well as higher fusion rates of lumbar spinal fusions *in vivo*, has been shown previously with

locally administered insulin<sup>14,95-97</sup>, as described earlier. The literature review presented herein and the studies included in this thesis, emphasises that locally delivered insulin has osteoinductive capacity, both in healthy and compromised animal models.

The clinical outcome, when a surgical intervention is needed, is dependent upon multiple factors, such as those related to the patient, surgeon, and materials used. With increased awareness of treatment choices, improved patient compliance, enhanced experience of the surgeon, optimised surgical techniques, and improvements to the applied materials, the majority of patients are today successfully treated. Those patients in greatest need of improvements are those with more severely compromised conditions. Therefore, pre-clinical efforts should be taken in account, to expand the possibilities to help a greater range of patients. However, previous reports have questioned the clinical relevance of animal findings<sup>152</sup>. Whether or not the enhancement of bone formation by local insulin delivery shown here for rats can be replicated in humans is an issue that needs to be further explored.

## 6 CONCLUSIONS

- I. It is concluded that insulin immobilised on a titanium implant surface and administered locally to non-diabetic subjects has the potential to increase bone formation.
- I. It is concluded that titanium surfaces can act as carriers for the hormone insulin. The insulin is released from the surface with preserved biological activity, *in vitro*. The decreased release of insulin with prolonged storage time needs to be considered when the implants are used in clinical situations.
- II. It is concluded that in spite of insulin release, the remaining coated layer has a stabilizing effect on the structures of other adsorbed proteins and supports the accumulation of calcium and phosphate ions at the interface.
- III. It is concluded that locally delivered insulin is a potential agent for enhanced bone formation with possible anti-inflammatory capacity in osteoporotic rats.

The overall conclusion is that insulin-coated titanium implants represent a potentially novel therapy for local bone regeneration, opening possibilities for new applications. However, the current immobilization technique has limitations, such as problems associated with controlling the concentration of bonded insulin and prolonged storage of the insulin-coated titanium implants.

## 7 REFERENCES

1. Adell R, Lekholm U, Rockler B, Branemark PI. A 15-year study of osseointegrated implants in the treatment of the edentulous jaw. *Int J Oral Surg* 1981;10(6):387-416.
2. Friberg B, Jemt T. Clinical experience of TiUnite implants: a 5-year cross-sectional, retrospective follow-up study. *Clin Implant Dent Relat Res* 2010;12 Suppl 1:e95-103.
3. Tjellstrom A, Hakansson B, Lindstrom J, Branemark PI, Hallen O, Rosenhall U, Leijon A. Analysis of the mechanical impedance of bone-anchored hearing aids. *Acta Otolaryngol* 1980;89(1-2):85-92.
4. Albrektsson T, Carlsson LV, Jacobsson M, Macdonald W. Gothenburg osseointegrated hip arthroplasty. Experience with a novel type of hip design. *Clin Orthop Relat Res* 1998(352):81-94.
5. Branemark R, Berlin O, Hagberg K, Bergh P, Gunterberg B, Rydevik B. A novel osseointegrated percutaneous prosthetic system for the treatment of patients with transfemoral amputation: A prospective study of 51 patients. *Bone Joint J* 2014;96-B(1):106-13.
6. Champy M, Lodde JP, Schmitt R, Jaeger JH, Muster D. Mandibular osteosynthesis by miniature screwed plates via a buccal approach. *J Maxillofac Surg* 1978;6(1):14-21.
7. Widar F. On factors influencing the clinical outcome in orthognathic surgery. Gothenburg: Univeristy of Gothenburg; 2015.
8. Derks J, Hakansson J, Wennstrom JL, Tomasi C, Larsson M, Berglundh T. Effectiveness of implant therapy analyzed in a Swedish population: early and late implant loss. *J Dent Res* 2015;94(3 Suppl):44S-51S.
9. Garellick GR, C. Kärrholm, J. Rolfson, O. The Swedish Hip Arthroplasty Register, Annual Reposrt 2012. . The Swedish Hip Arthroplasty Register, Anual Report; 2012.
10. Mohaddes M. Acetabular Revisions Risk Factors & Prediction of Re-revision: University of Gothenburg; 2015.
11. Bojan. A.J. Tochanteric Hip Fractures. Clinicial outcomes and the cut-out complication. Gothenburg: Univeristy of Gothenburg; 2014.
12. Steinmann JC, Herkowitz HN. Pseudarthrosis of the spine. *Clin Orthop Relat Res* 1992(284):80-90.
13. Gruskay JA, Webb ML, Grauer JN. Methods of evaluating lumbar and cervical fusion. *Spine J* 2014;14(3):531-9.
14. Koerner JD, Yalamanchili P, Munoz W, Uko L, Chaudhary SB, Lin SS, Vives MJ. The effects of local insulin application to lumbar spinal fusions in a rat model. *Spine J* 2013;13(1):22-31.

15. Buser DD, C. Schenk, R. . Guided Bone Regeneration in Implant Dent. New Malden: Quintessence Publishin; 1994. 270 p.
16. Buckwalter JA, Glimcher MJ, Cooper RR, Recker R. Bone biology. I: Structure, blood supply, cells, matrix, and mineralization. Instr Course Lect 1996;45:371-86.
17. Marieb EN. Human Anatomy & Physiology, Fifth edition: Benjamin Cummings; 2001.
18. Berglund GE-L, A. Lindgren, S. Lindholm, N. . Med. Internmedicin. Stockholm: Liber AB; 2009.
19. Florencio-Silva R, Sasso GR, Sasso-Cerri E, Simoes MJ, Cerri PS. Biology of Bone Tissue: Structure, Function, and Factors That Influence Bone Cells. Biomed Res Int 2015;2015:421746.
20. Sims NA, Martin TJ. Coupling the activities of bone formation and resorption: a multitude of signals within the basic multicellular unit. Bonekey Rep 2014;3:481.
21. Lerner UHM, D. Behandlingsprinciper för olika läkemedel vid osteoporos. Tandläkartidningen 2012;104(11):64-78.
22. Lerner UHL, Ö. Benvävnadens omsättning. Tandläkartidningen 2006;4(103):2972-2975.
23. Raggatt LJ, Partridge NC. Cellular and molecular mechanisms of bone remodeling. J Biol Chem 2010;285(33):25103-8.
24. Roberts SJ, van Gestel N, Carmeliet G, Luyten FP. Uncovering the periosteum for skeletal regeneration: the stem cell that lies beneath. Bone 2015;70:10-8.
25. Ozaki A, Tsunoda M, Kinoshita S, Saura R. Role of fracture hematoma and periosteum during fracture healing in rats: interaction of fracture hematoma and the periosteum in the initial step of the healing process. J Orthop Sci 2000;5(1):64-70.
26. Downey PA, Siegel MI. Bone biology and the clinical implications for osteoporosis. Phys Ther 2006;86(1):77-91.
27. Robling C, Turner. Basic Bone Biology. Annu. Rev. Biomed. Eng 2006;8:455-498.
28. Robling AG, Castillo AB, Turner CH. Biomechanical and molecular regulation of bone remodeling. Annu Rev Biomed Eng 2006;8:455-98.
29. Long F. Building strong bones: molecular regulation of the osteoblast lineage. Nat Rev Mol Cell Biol 2011;13(1):27-38.
30. Nakamura H. Morphology, function and differentiation of bone cells. Journal of Hard Tissue Biology 2007;16(1):15-22.
31. Lerner UH, Ohlsson C. The WNT system: background and its role in bone. J Intern Med 2015;DOI:10.1111/joim.12368.
32. Clarke B. Normal bone anatomy and physiology. Clin J Am Soc Nephrol 2008;3 Suppl 3:S131-9.

33. Lerner UH, Ljunggren O. [Bone remodeling]. *Lakartidningen* 2006;103(40):2972-5.
34. Kon T, Cho TJ, Aizawa T, Yamazaki M, Nooh N, Graves D, Gerstenfeld LC, Einhorn TA. Expression of osteoprotegerin, receptor activator of NF-kappaB ligand (osteoprotegerin ligand) and related proinflammatory cytokines during fracture healing. *J Bone Miner Res* 2001;16(6):1004-14.
35. Millan JL. The role of phosphatases in the initiation of skeletal mineralization. *Calcif Tissue Int* 2013;93(4):299-306.
36. Puskas J. Introduction to polymer chemistry. A biobased approach. USA: DEStech Publication Inc; 2014.
37. Lerner UL, P. Brechter, A. Palmqvist, P. Persson, E. Skelettet vid hälsa och sjukdom. *Tandläkartidningen* 2008;100(5):84-90.
38. Lewiecki EM. New targets for intervention in the treatment of postmenopausal osteoporosis. *Nat Rev Rheumatol* 2011;7(11):631-8.
39. Dimitriou R, Tsiridis E, Giannoudis PV. Current concepts of molecular aspects of bone healing. *Injury* 2005;36(12):1392-404.
40. Marco F, Milena F, Gianluca G, Vittoria O. Peri-implant osteogenesis in health and osteoporosis. *Micron* 2005;36(7-8):630-44.
41. Anderson JM, Rodriguez A, Chang DT. Foreign body reaction to biomaterials. *Semin Immunol* 2008;20(2):86-100.
42. Ehrnthaller C, Huber-Lang M, Nilsson P, Bindl R, Redeker S, Recknagel S, Rapp A, Mollnes T, Amling M, Gebhard F and others. Complement C3 and C5 deficiency affects fracture healing. *PLoS One* 2013;8(11):e81341.
43. Huber-Lang M, Kovtun A, Ignatius A. The role of complement in trauma and fracture healing. *Semin Immunol* 2013;25(1):73-8.
44. Omar O, Lenneras M, Svensson S, Suska F, Emanuelsson L, Hall J, Nannmark U, Thomsen P. Integrin and chemokine receptor gene expression in implant-adherent cells during early osseointegration. *J Mater Sci Mater Med* 2010;21(3):969-80.
45. Brånemark R. A biomechanical study of osseointegration. Sweden: University of Gothenburg; 1996.
46. Oni O. Callus formation during diaphyseal fracture repair. *Orthopaedics international edition* 1996;4(4):269-277.
47. Lerner UH. Skelettet i käkar och annorstädes. *Tandläkartidningen* 2006;98(15):50-61.
48. Jonsson E, Eriksson D, Akesson K, Ljunggren O, Salomonsson S, Borgstrom F, Strom O. Swedish osteoporosis care. *Arch Osteoporos* 2015;10:222.

49. Hollinger JO, Winn S, Bonadio J. Options for tissue engineering to address challenges of the aging skeleton. *Tissue Eng* 2000;6(4):341-50.
50. Thomas DMN, W. K. Best, D. B. Insulin and Bone: A clinical and Scientific Review. *Endocrinology and Metabolism* 1997;4:5-17.
51. Bouillon R. Diabetic bone disease. *Calcif Tissue Int* 1991;49(3):155-60.
52. Thrailkill KM, Lumpkin CK, Jr., Bunn RC, Kemp SF, Fowlkes JL. Is insulin an anabolic agent in bone? Dissecting the diabetic bone for clues. *Am J Physiol Endocrinol Metab* 2005;289(5):E735-45.
53. Kayal RA, Alblowi J, McKenzie E, Krothapalli N, Silkman L, Gerstenfeld L, Einhorn TA, Graves DT. Diabetes causes the accelerated loss of cartilage during fracture repair which is reversed by insulin treatment. *Bone* 2009;44(2):357-63.
54. Kemink SA, Hermus AR, Swinkels LM, Lutterman JA, Smals AG. Osteopenia in insulin-dependent diabetes mellitus; prevalence and aspects of pathophysiology. *J Endocrinol Invest* 2000;23(5):295-303.
55. Kawashima Y, Fritton JC, Yakar S, Epstein S, Schaffler MB, Jepsen KJ, LeRoith D. Type 2 diabetic mice demonstrate slender long bones with increased fragility secondary to increased osteoclastogenesis. *Bone* 2009;44(4):648-55.
56. Jiao H, Xiao E, Graves DT. Diabetes and Its Effect on Bone and Fracture Healing. *Curr Osteoporos Rep* 2015;13(5):327-35.
57. Pietschmann P, Patsch JM, Schernthaner G. Diabetes and bone. *Horm Metab Res* 2010;42(11):763-8.
58. Gupte AA, Pownall HJ, Hamilton DJ. Estrogen: an emerging regulator of insulin action and mitochondrial function. *J Diabetes Res* 2015;2015:916585.
59. Bryzgalova G, Gao H, Ahren B, Zierath JR, Galuska D, Steiler TL, Dahlman-Wright K, Nilsson S, Gustafsson JA, Efendic S and others. Evidence that oestrogen receptor-alpha plays an important role in the regulation of glucose homeostasis in mice: insulin sensitivity in the liver. *Diabetologia* 2006;49(3):588-97.
60. Löfman O. Epidemiologin för frakturer. *Läkartidningen* 2006;103(40).
61. Kanis JA, Oden A, McCloskey EV, Johansson H, Wahl DA, Cooper C, Epidemiology IOFWGo, Quality of L. A systematic review of hip fracture incidence and probability of fracture worldwide. *Osteoporos Int* 2012;23(9):2239-56.
62. Pesce V, Speciale D, Sammarco G, Patella S, Spinarelli A, Patella V. Surgical approach to bone healing in osteoporosis. *Clin Cases Miner Bone Metab* 2009;6(2):131-5.

63. Chrcanovic BR, Albrektsson T, Wennerberg A. Diabetes and oral implant failure: a systematic review. *J Dent Res* 2014;93(9):859-67.
64. Goldhahn J, Suhm N, Goldhahn S, Blauth M, Hanson B. Influence of osteoporosis on fracture fixation--a systematic literature review. *Osteoporos Int* 2008;19(6):761-72.
65. Mellado-Valero A, Ferrer-Garcia JC, Calvo-Catala J, Labaig-Rueda C. Implant treatment in patients with osteoporosis. *Med Oral Patol Oral Cir Bucal* 2010;15(1):e52-7.
66. Guobis Z, Pacauskiene I, Astramskaite I. General Diseases Influence on Peri-Implantitis Development: a Systematic Review. *J Oral Maxillofac Res* 2016;7(3):e5.
67. Duckworth WC, Bennett RG, Hamel FG. Insulin degradation: progress and potential. *Endocr Rev* 1998;19(5):608-24.
68. Thomas DM, Udagawa N, Hards DK, Quinn JM, Moseley JM, Findlay DM, Best JD. Insulin receptor expression in primary and cultured osteoclast-like cells. *Bone* 1998;23(3):181-6.
69. Pun KK, Lau P, Ho PW. The characterization, regulation, and function of insulin receptors on osteoblast-like clonal osteosarcoma cell line. *J Bone Miner Res* 1989;4(6):853-62.
70. Fulzele K, Riddle RC, DiGirolamo DJ, Cao X, Wan C, Chen D, Faugere MC, Aja S, Hussain MA, Bruning JC and others. Insulin receptor signaling in osteoblasts regulates postnatal bone acquisition and body composition. *Cell* 2010;142(2):309-19.
71. Levy RM, E. Manolagas, S. Olefsky, MJ. Demonstration fo insulin receptors and modulation of alkanin phosphatase activity by insulin in rat osteoblastic cells. *Endocrinology* 1986;119(4):1786-1792.
72. Lee J, Pilch PF. The insulin receptor: structure, function, and signaling. *Am J Physiol* 1994;266(2 Pt 1):C319-34.
73. Blundell TL, Cutfield JF, Dodson EJ, Dodson GG, Hodgkin DC, Mercola DA. The crystal structure of rhombohedral 2 zinc insulin. *Cold Spring Harb Symp Quant Biol* 1972;36:233-41.
74. Chang X, Jorgensen AM, Bardrum P, Led JJ. Solution structures of the R6 human insulin hexamer. *Biochemistry* 1997;36(31):9409-22.
75. Yang J, Zhang X, Wang W, Liu J. Insulin stimulates osteoblast proliferation and differentiation through ERK and PI3K in MG-63 cells. *Cell Biochem Funct* 2010;28(4):334-41.
76. Taniguchi CM, Emanuelli B, Kahn CR. Critical nodes in signalling pathways: insights into insulin action. *Nat Rev Mol Cell Biol* 2006;7(2):85-96.
77. Zhang W, Shen X, Wan C, Zhao Q, Zhang L, Zhou Q, Deng L. Effects of insulin and insulin-like growth factor 1 on osteoblast proliferation and differentiation: differential signalling via Akt and ERK. *Cell Biochem Funct* 2012;30(4):297-302.

78. Entingh-Pearsall A, Kahn CR. Differential roles of the insulin and insulin-like growth factor-I (IGF-I) receptors in response to insulin and IGF-I. *J Biol Chem* 2004;279(36):38016-24.
79. Fulzele K, DiGirolamo DJ, Liu Z, Xu J, Messina JL, Clemens TL. Disruption of the insulin-like growth factor type 1 receptor in osteoblasts enhances insulin signaling and action. *J Biol Chem* 2007;282(35):25649-58.
80. Li S, Leblanc RM. Aggregation of insulin at the interface. *J Phys Chem B* 2014;118(5):1181-8.
81. Fulzele K, Clemens TL. Novel functions for insulin in bone. *Bone* 2012;50(2):452-6.
82. Sun Q, Li J, Gao F. New insights into insulin: The anti-inflammatory effect and its clinical relevance. *World J Diabetes* 2014;5(2):89-96.
83. Li J, Zhang H, Wu F, Nan Y, Ma H, Guo W, Wang H, Ren J, Das UN, Gao F. Insulin inhibits tumor necrosis factor-alpha induction in myocardial ischemia/reperfusion: role of Akt and endothelial nitric oxide synthase phosphorylation. *Crit Care Med* 2008;36(5):1551-8.
84. Dandona P, Aljada A, Mohanty P, Ghanim H, Hamouda W, Assian E, Ahmad S. Insulin inhibits intranuclear nuclear factor kappaB and stimulates IkappaB in mononuclear cells in obese subjects: evidence for an anti-inflammatory effect? *J Clin Endocrinol Metab* 2001;86(7):3257-65.
85. Zhao WQ, Alkon DL. Role of insulin and insulin receptor in learning and memory. *Mol Cell Endocrinol* 2001;177(1-2):125-34.
86. Craft S, Newcomer J, Kanne S, Dagogo-Jack S, Cryer P, Sheline Y, Luby J, Dagogo-Jack A, Alderson A. Memory improvement following induced hyperinsulinemia in Alzheimer's disease. *Neurobiol Aging* 1996;17(1):123-30.
87. Ferron M, Wei J, Yoshizawa T, Del Fattore A, DePinho RA, Teti A, Ducy P, Karsenty G. Insulin signaling in osteoblasts integrates bone remodeling and energy metabolism. *Cell* 2010;142(2):296-308.
88. Clemens TL, Karsenty G. The osteoblast: an insulin target cell controlling glucose homeostasis. *J Bone Miner Res* 2011;26(4):677-80.
89. Li H, Liu D, Zhao CQ, Jiang LS, Dai LY. Insulin potentiates the proliferation and bone morphogenetic protein-2-induced osteogenic differentiation of rat spinal ligament cells via extracellular signal-regulated kinase and phosphatidylinositol 3-kinase. *Spine (Phila Pa 1976)* 2008;33(22):2394-402.
90. Huang S, Kaw M, Harris MT, Ebraheim N, McInerney MF, Najjar SM, Lecka-Czernik B. Decreased osteoclastogenesis and high bone mass in mice with impaired insulin clearance due to liver-specific inactivation to CEACAM1. *Bone* 2010;46(4):1138-45.

91. Bosetti M, Sabbatini M, Nicoli E, Fusaro L, Cannas M. Effects and differentiation activity of IGF-I, IGF-II, insulin and preptin on human primary bone cells. *Growth Factors* 2013;31(2):57-65.
92. Cornish J, Callon KE, Reid IR. Insulin increases histomorphometric indices of bone formation In vivo. *Calcif Tissue Int* 1996;59(6):492-5.
93. Stuck WG. The effect of Insulin on the healing of experimental fractures in the rabbit. *J Bone Joint Surg Am* 1932;14(1):109-115.
94. Gandhi A, Beam HA, O'Connor JP, Parsons JR, Lin SS. The effects of local insulin delivery on diabetic fracture healing. *Bone* 2005;37(4):482-90.
95. Dedania J, Borzio R, Paglia D, Breitbart EA, Mitchell A, Vaidya S, Wey A, Mehta S, Benevenia J, O'Connor JP and others. Role of local insulin augmentation upon allograft incorporation in a rat femoral defect model. *J Orthop Res* 2011;29(1):92-9.
96. Paglia DN, Wey A, Breitbart EA, Faiwyszewski J, Mehta SK, Al-Zube L, Vaidya S, Cottrell JA, Graves D, Benevenia J and others. Effects of local insulin delivery on subperiosteal angiogenesis and mineralized tissue formation during fracture healing. *J Orthop Res* 2013;31(5):783-91.
97. Park AG, Paglia DN, Al-Zube L, Hreha J, Vaidya S, Breitbart E, Benevenia J, O'Connor JP, Lin SS. Local insulin therapy affects fracture healing in a rat model. *J Orthop Res* 2013;31(5):776-82.
98. Hrynyk M, Martins-Green M, Barron AE, Neufeld RJ. Sustained prolonged topical delivery of bioactive human insulin for potential treatment of cutaneous wounds. *Int J Pharm* 2010;398(1-2):146-54.
99. Han Y, Zhang X, Lingling E, Wang D, Liu H. Sustained local delivery of insulin for potential improvement of peri-implant bone formation in diabetes. *Sci China Life Sci* 2012;55(11):948-57.
100. Wang B, Song Y, Wang F, Li D, Zhang H, Ma A, Huang N. Effects of local infiltration of insulin around titanium implants in diabetic rats. *Br J Oral Maxillofac Surg* 2011;49(3):225-9.
101. Williams DF. Implants in dental and maxillofacial surgery. *Biomaterials* 1981;2(3):133-46.
102. Kasemo B. Biocompatibility of titanium implants: surface science aspects. *J Prosthet Dent* 1983;49(6):832-7.
103. Albrektsson T, Branemark PI, Hansson HA, Lindstrom J. Osseointegrated titanium implants. Requirements for ensuring a long-lasting, direct bone-to-implant anchorage in man. *Acta Orthop Scand* 1981;52(2):155-70.
104. Sundell G, Dahlin C, Andersson M, Thuvander M. The bone-implant interface of dental implants in humans on the atomic scale. *Acta Biomater* 2017;48:445-450.

105. Guilherme AS, Henriques GE, Zavanelli RA, Mesquita MF. Surface roughness and fatigue performance of commercially pure titanium and Ti-6Al-4V alloy after different polishing protocols. *J Prosthet Dent* 2005;93(4):378-85.
106. Palmquist A, Lindberg F, Emanuelsson L, Branemark R, Engqvist H, Thomsen P. Morphological studies on machined implants of commercially pure titanium and titanium alloy (Ti6Al4V) in the rabbit. *J Biomed Mater Res B Appl Biomater* 2009;91(1):309-19.
107. Almasi D, Izman S, Sadeghi M, Iqbal N, Roozbahani F, Krishnamurthy G, Kamarul T, Abdul Kadir MR. In vitro evaluation of bioactivity of chemically deposited hydroxyapatite on polyether ether ketone. *Int J Biomater* 2015;2015:475435.
108. Albrektsson T, Dahlin C, Jemt T, Sennerby L, Turri A, Wennerberg A. Is marginal bone loss around oral implants the result of a provoked foreign body reaction? *Clin Implant Dent Relat Res* 2014;16(2):155-65.
109. Göransson A. On Possibly Bioactive CP Titanium Implant Surface. Sweden, Gothenburg: Gothenburgs University; 2006. ISBN:10:91-628-7005-X p.
110. Wennerberg A, Albrektsson T. Effects of titanium surface topography on bone integration: a systematic review. *Clin Oral Implants Res* 2009;20 Suppl 4:172-84.
111. Albrektsson T, Wennerberg A. Oral implant surfaces: Part 1--review focusing on topographic and chemical properties of different surfaces and in vivo responses to them. *Int J Prosthodont* 2004;17(5):536-43.
112. Wennerberg A, Albrektsson T. Suggested guidelines for the topographic evaluation of implant surfaces. *Int J Oral Maxillofac Implants* 2000;15(3):331-44.
113. Wennerberg A. On surface roughness and implant incorporation. . Sweden: University of Gothenburg; 1996.
114. Rasmusson L, Roos J, Bystedt H. A 10-year follow-up study of titanium dioxide-blasted implants. *Clin Implant Dent Relat Res* 2005;7(1):36-42.
115. Albrektsson T, Wennerberg A. Oral implant surfaces: Part 2--review focusing on clinical knowledge of different surfaces. *Int J Prosthodont* 2004;17(5):544-64.
116. Svanborg LM, Andersson M, Wennerberg A. Surface characterization of commercial oral implants on the nanometer level. *J Biomed Mater Res B Appl Biomater* 2010;92(2):462-9.
117. Glauser R, Ruhstaller P, Windisch S, Zembic A, Lundgren A, Gottlow J, Hammerle CH. Immediate occlusal loading of Branemark System TiUnite implants placed predominantly in soft bone: 4-year

- results of a prospective clinical study. *Clin Implant Dent Relat Res* 2005;7 Suppl 1:S52-9.
118. Horbett TA. Principles underlying the role of adsorbed plasma proteins in blood interactions with foreign materials. *Cardiovasc Pathol* 1993;2:137-148.
  119. Arvidsson S, Askendal A, Tengvall P. Blood plasma contact activation on silicon, titanium and aluminium. *Biomaterials* 2007;28(7):1346-54.
  120. Castner GDBDR. Biomedical surface science: Foundation to frontiers. *Surface Science* 2001;500:28-60.
  121. Vogler EA. Protein adsorption in three dimensions. *Biomaterials* 2012;33(5):1201-37.
  122. Shchukarev AR, M. Mladenovic, Z. To Build or Not to Build: The Interface of Bone Graft Substitute Materials in Biological Media from the View Point of the Cells. In: Pignatello PR, editor. *Biomaterials Science and Engineering: InTeck*; 2011.
  123. Stenport VF, Johansson C, Heo SJ, Aspenberg P, Albrektsson T. Titanium implants and BMP-7 in bone: an experimental model in the rabbit. *J Mater Sci Mater Med* 2003;14(3):247-54.
  124. Schmidmaier G, Lucke M, Schwabe P, Raschke M, Haas NP, Wildemann B. Collective review: bioactive implants coated with poly(D,L-lactide) and growth factors IGF-I, TGF-beta1, or BMP-2 for stimulation of fracture healing. *J Long Term Eff Med Implants* 2006;16(1):61-9.
  125. Wermelin K, Aspenberg P, Linderback P, Tengvall P. Bisphosphonate coating on titanium screws increases mechanical fixation in rat tibia after two weeks. *J Biomed Mater Res A* 2008;86(1):220-7.
  126. Dettin M, Bagno A, Gambaretto R, Iucci G, Conconi MT, Tuccitto N, Menti AM, Grandi C, Di Bello C, Licciardello A and others. Covalent surface modification of titanium oxide with different adhesive peptides: surface characterization and osteoblast-like cell adhesion. *J Biomed Mater Res A* 2009;90(1):35-45.
  127. Gautschi OP, Frey SP, Zellweger R. Bone morphogenetic proteins in clinical applications. *ANZ J Surg* 2007;77(8):626-31.
  128. Olde Damink LH, Dijkstra PJ, van Luyn MJ, van Wachem PB, Nieuwenhuis P, Feijen J. Cross-linking of dermal sheep collagen using a water-soluble carbodiimide. *Biomaterials* 1996;17(8):765-73.
  129. Tengvall. P JE, Askendal. A, Thomsen. P, Gretzer. C. Preparation of multilayer plasma protein films on silicon by EDC/NHS coupling chemistry. *Colloids and Surfaces B: Biointerfaces* 2003;28(4):261-272.

130. Wermelin K, Suska F, Tengvall P, Thomsen P, Aspenberg P. Stainless steel screws coated with bisphosphonates gave stronger fixation and more surrounding bone. *Histomorphometry in rats*. *Bone* 2008;42(2):365-71.
131. Hermanson TKM, A. Smith, KP. Immobilized affinity ligand techniques. London: Academic Press, Inc.; 1992.
132. Sul YT, Johansson CB, Albrektsson T. Oxidized titanium screws coated with calcium ions and their performance in rabbit bone. *Int J Oral Maxillofac Implants* 2002;17(5):625-34.
133. Tengvall P, Jansson E, Askendal A, Thomsen P, Gretzer C. Preparation of multilayer plasma protein films by EDS/NHS coupling chemistry on silicon. *Colloids Surf B Biointerfaces* 2003;28(4):261-72.
134. Malekzadeh BT, P. Öhrnell, L-O. Wennerberg, A. Westerlund-Göransson, A. Effect of local insulin administration on bone formation in non-diabetic rat. *J Biomed Mater Res A* 2012:under revision.
135. McCrackin. F. L. A Fortran program for the analysis of ellipsometer measurements. . Washington DC: NBS Technical Note 479; 1969.
136. de Feijter. J.A BJ, Veer. F.A. Ellipsometry as a toll to study the adsorption of synthetic and biopolymers at the air-water interface. *Biopolymers* 1978;17:1759-1773.
137. Benesch. J AA, Tengvall. T. Quantification of adsorbed human serum albumin at solid interface: a comparison between radioimmunoassay (RIA) and simple null ellipsometry. *Colloids Surf B: Biointerfaces* 2000:71-81.
138. Stenberg. M NH. The use of the isoscopoe ellipsometer in the study of adsorbed proteins and biospecific binding reactions. *J Phys* 1983;C10(12):83-86.
139. Pautke C, Schieker M, Tischer T, Kolk A, Neth P, Mutschler W, Milz S. Characterization of osteosarcoma cell lines MG-63, Saos-2 and U-2 OS in comparison to human osteoblasts. *Anticancer Res* 2004;24(6):3743-8.
140. Repetto G, del Peso A, Zurita JL. Neutral red uptake assay for the estimation of cell viability/cytotoxicity. *Nat Protoc* 2008;3(7):1125-31.
141. Stanford CM, Jacobson PA, Eanes ED, Lembke LA, Midura RJ. Rapidly forming apatitic mineral in an osteoblastic cell line (UMR 106-01 BSP). *J Biol Chem* 1995;270(16):9420-8.
142. Gregory CA, Gunn WG, Peister A, Prockop DJ. An Alizarin red-based assay of mineralization by adherent cells in culture: comparison with cetylpyridinium chloride extraction. *Anal Biochem* 2004;329(1):77-84.

143. Thompson DD, Simmons HA, Pirie CM, Ke HZ. FDA Guidelines and animal models for osteoporosis. *Bone* 1995;17(4 Suppl):125S-133S.
144. Johnston BD, Ward WE. The ovariectomized rat as a model for studying alveolar bone loss in postmenopausal women. *Biomed Res Int* 2015;2015:635023.
145. Altman RD, Latta LL, Keer R, Renfree K, Hornicek FJ, Banovac K. Effect of nonsteroidal antiinflammatory drugs on fracture healing: a laboratory study in rats. *J Orthop Trauma* 1995;9(5):392-400.
146. Lerner UH. Inflammation-induced bone remodeling in periodontal disease and the influence of post-menopausal osteoporosis. *J Dent Res* 2006;85(7):596-607.
147. Lerner UH. Bone remodeling in post-menopausal osteoporosis. *J Dent Res* 2006;85(7):584-95.
148. Cammarata CR, Hughes ME, Ofner CM, 3rd. Carbodiimide induced cross-linking, ligand addition, and degradation in gelatin. *Mol Pharm* 2015;12(3):783-93.
149. Malekzadeh BO, Ransjo M, Tengvall P, Mladenovic Z, Westerlund A. Insulin released from titanium discs with insulin coatings-Kinetics and biological activity. *J Biomed Mater Res B Appl Biomater* 2016.
150. Ellingsen JE. Surface configurations of dental implants. *Periodontol* 2000 1998;17:36-46.
151. Malekzadeh B, Tengvall P, Ohrnell LO, Wennerberg A, Westerlund A. Effects of locally administered insulin on bone formation in non-diabetic rats. *J Biomed Mater Res A* 2013;101(1):132-7.
152. Ivanoff C-J. On surgical and implant related factors influencing integration and function of titanium implants. Sweden: University of Gothenburg; 1999.

## 8 ACKNOWLEDGEMENTS

This thesis was carried out in co-operation with the Department of Orthodontics (Institute of Odontology, University of Gothenburg) and the Department of Biomaterials (Institute of Clinical Sciences, University of Gothenburg). I wish to express my sincerest appreciation and gratitude to all who have been involved in this research, with special thanks to:

### **My supervisors**

Associate Professor and main supervisor Anna Westerlund, who initiated this project: Thank you for your never-ending enthusiasm, encouragement, and excellent scientific guidance. Furthermore, thank you for sharing your expansive knowledge of surface science and for your great attention to detail. You are a genuine friend who between times reminded me of the importance of achieving a balance between work and family life. You are a true fighter and a great role model.

Professor and co-supervisor Maria Ransjö: Thank you for sharing your profound knowledge on bone biology, and for your constructive criticisms and valuable discussions. Furthermore, thank you for introducing me to cellular laboratory work, thereby adding a greater dimension to my education.

Professor and co-supervisor Pentti Tengvall: Thank you for giving me the opportunity to join your department, and for sharing your profound experiences regarding immobilization techniques and osseointegration. You encourage your students' curiosity and foster the possibility for innovations to take place in this contemporary controlled, and sometimes inhibiting academic environment. You are a true professor.

### **My co-authors**

Ann Wennerberg, for creating the possibility for me to start pursuing scientific research and for your support in Studies I, II and IV.

Zivko Mladenovic, for introducing me to the cell laboratory and for your guidance and efforts in Study II.

Andrey Shchukarev, for sharing your priceless expertise regarding XPS and proteins at interfaces, as well as for making Study III possible.

Anders Palmquist, for sharing your great experiences and providing kind assistance with the SEM. Furthermore, for your guidance in Study IV.

Malin Erlandsson and Maria Bokarewa, for all your contributions regarding the micro-CT evaluations and guidance in Study IV.

## **My supporters**

Göran Widmark, for creating the possibility to combine my clinical work with this research project. You have always supported me and encouraged me to go further. Thank you.

Lena Emanuelsson and Petra Johansson, for all the valuable advice, help with the animal experiments, and preparation of the samples, as well as lots of laughter and kindness. Your helpfulness and great experience have eased many stressful days.

Ann-Sophie Corneliusson, for your great assistance with the animal surgeries.

Pamela Uribe and Lena Larsson, for your valuable guidance and help in the cell laboratory.

Maria Lennerås, for advice regarding the quantitative Real-Time PCR experiments and your kindness.

Sandra Ståhlberg, for always being helpful in administrative matters and proof reading.

## **My family**

My mother Pouran and my father Heidar. Thank you for your generous LOVE and continuous support, and for raising me to believe that nothing is impossible, the only limitation being my own imagination. You give me emotional security and confidence. I cannot imagine a life without the two of you.

My life companion Lars-Olof. Thank you for making this project possible by your never-ending support and tremendous patience. Thank you for sharing your life experience and always pushing me to go further. You bring me courage and nothing in life is threatening with you by my side. I love you to the moon and back! And finally, thank you for bringing me the great gift in life, Arwin.

## **For financial support, I want to thank:**

Stiftelsen Handlanden Hjalmar Svenssons forskningsfond, Kungliga och Hvitfeldtska Stiftelsen, Doktor Felix Neuberghs Stiftelse, Göteborgs Diabetesförening.

